UNIVERSITY OF OKLAHOMA

GRADUATE COLLEGE

DATA-BASED STOCHASTIC NETWORK MITIGATION

A THESIS

SUBMITTED TO THE GRADUATE FACULTY

in partial fulfillment of the requirements for the

Degree of

MASTER OF SCIENCE

By

ALEXANDER D. RODRIGUEZ CASTILLO
Norman, Oklahoma
2018

DATA-BASED STOCHASTIC NETWORK MITIGATION

A THESIS APPROVED FOR THE
GALLOGLY COLLEGE OF ENGINEERING

BY

Dr. Charles D. Nicholson, Chair

Dr. Amy McGovern

Dr. Naiyu Wang

To my parents for their support and motivation to pursue my dreams

Acknowledgments

This thesis subsumes some novel ideas that came out from discussions with Dr. Charles D. Nicholson, a lovely person whom I had the honor to have as advisor. Thanks to our close collaboration, I am a more mature prospective researcher. I greatly appreciate the trust he placed on me to work in independent research since the beginning of my studies. And most importantly, I want to express my deepest gratitude for his genuine care and support on my personal wellbeing and future career.

I want to thank Dr. Naiyu Wang and Dr. Amy McGovern for acceding to be my committee members. Both of them gave me comments to improve this work since its early stages. Dr. Wang was very kind in letting me join her laboratory, which is co-directed with Dr. Nicholson. It was a thought provoking space with great individuals working in novel ideas. Dr. McGovern kindly provided me career advice for my future career path, which I greatly appreciate.

I must also thank my fellow colleagues at the NIST-funded Community Resilience Laboratory, the Data Analytics Laboratory and the Systems Realization Laboratory. We shared not only ideas and knowledge, but also memorable and joyful moments that forged our friendship.

From inside and outside the academic environment, first as an exchange student and then as a master student, I made several close friends at Oklahoma. I want to deeply thank each for giving me some of the best of them.

Finally, I would like to give the most heart felt gratitude to my family and significant other. They made real sacrifices for me to achieve my goals, from which I am deeply thankful.

Contents

1 Introduction **1**

2 Background **4**

2.1 Component Importance Measures (CIMs) 6

2.2 Stochastic Network Design (SND) 7

2.3 Uncertainty and Complexity of Network Failures 8

3 Incorporating Failure Uncertainty in CIMs **12**

3.1 CIM-based decision-making 12

3.1.1 CIM Definitions 12

3.1.2 Probabilistic Delta Centrality 15

3.2 Case Study 16

3.2.1 Analysis with the Probabilistic Delta Centrality 17

3.3 Concluding Remarks 20

4 Incorporating Failure Complexity in SND **22**

4.1 Adapting SND to Mitigation 23

4.2 Data-based Stochastic Network Mitigation 25

4.2.1 Simulation-based data generation 26

4.2.2 Probabilistic data transformation 27

4.2.3 Statistical modeling 29

4.2.4 Optimization formulation 30

4.2.5 Correction of expected performance metric value 31

5 Example 1: Shelby County Transportation Network **34**

5.1 Scenario Setup 34

5.2 Application of Methodology 36

5.2.1 Data Generation and Transformation 36

5.2.2 Statistical Modeling 37
5.2.3 Optimization 42
5.2.4 Correction of Predicted Performance Metric $\hat{\varphi}_p$ 43
5.3 Results and Discussion 44

6 Example 2: IEEE 30-bus Test System **47**
6.1 Scenario Setup 47
6.2 Application of Methodology 51
6.2.1 Data Generation and Transformation 51
6.2.2 Statistical Modeling 52
6.2.3 Optimization 58
6.2.4 Correction of Predicted Performance Metric $\hat{\varphi}_p$ 59
6.3 Results and Discussion 60

7 Conclusions **63**

8 Future work **65**

References **66**

List of Tables

3.1 Top five components along with two other components that serve in the discussion. 18

3.2 Top five synergistic information centralities for combinations of two edges. 18

4.1 Example observations in realization dataset Ω. 27

4.2 Example observations in probabilistic dataset Ψ. 28

5.1 Hyper-parameter values considered in tunning the random forest. Selected in bold. 38

5.2 Genetic algorithm parameters. 42

5.3 Solutions for constrained cases with bridge indexes sorted by information centrality $C_i^{\Delta I}$. Each solution column contains the level of improvement suggested for each component i, from 0 (no improvement) to 4 (highest improvement). At the bottom, predicted average performance metric $\bar{\varphi}_p$ (objective) and corrected expected performance metric $\bar{\varphi}_c$ for each solution. 46

6.1 Component ID sorted by $C_i^{\Delta F}$. 51

6.2 Hyper-parameter values considered in tunning the random forest. Selected in bold. 54

6.3 Genetic algorithm parameters. 58

6.4 Solutions for constrained cases with component ID sorted by component type and index number. Each solution column contains the level of improvement suggested for each component. At the bottom, predicted average performance metric $\bar{\varphi}_p$ (objective) and corrected expected performance metric $\bar{\varphi}_c$ for each solution. Note that from the 71 components, only the ones that have improvements are presented. 61

List of Figures

1.1 Worldwide air transportation network [1]. It is an example of a network prone to costly disruptions. 2

2.1 Obstruction in highway. 5
2.2 Seismic retrofit for bridge using steel jackets in columns. Left: before retrofit; right: after retrofit. 6
2.3 Uncertainty and complexity in network failures. 9
2.4 Pros and cons of using SAA 11

3.1 The positive drop in the performance metric after disruption is denoted as (ΔP). 13
3.2 Random geometric graph of 200 nodes and 534 edges. Selected edge indexes are labeled. 17
3.3 Probabilistic information centrality as a function of failure probability p for select pairs of components. 19

4.1 Overview of the proposed methodology. 25
4.2 Multi-layer Monte Carlo Simulation (MCS). 26

5.1 Shelby County transportation network, only major highways depicted 35
5.2 Levels of improvement with associated survival probabilities and costs. 36
5.3 Histograms of component survival probabilities. Left, sampled with $\eta = 20$; right, sampled with $\eta = 40$. 37
5.4 Learning curve for random forest model before (above) and after (below) regularization. 40
5.5 Reliability curve for final random forest model. Gray dashed line is a perfect reliability curve. Red is actual. 41

6.1 Single-line diagram of the IEEE 30-bus test system [2]. 48

6.2 Graph representation of the IEEE 30-bus test system [2]. The dark grey nodes labeled with G represent the generator nodes, the white nodes labeled with T represent transmission nodes, and the light grey nodes labeled with D represent the demand nodes. 49
6.3 Levels of improvement with associated survival probabilities and costs for each type of component. 50
6.4 Histograms of component survival probabilities generated with $\eta = 35$ for each type of component. A: generator nodes; B: demand nodes; C: transmission node; D: transmission link. . . 53
6.5 Learning curve for random forest model before (above) and after (below) regularization. 56
6.6 Reliability curve for final random forest model. Gray dashed line is a perfect reliability curve. Red is actual. 57

Abstract

Current decision-support frameworks to assist mitigation planning do not include uncertainty and complexity of network failures, either one or both. To close this research gap, this thesis walks through a demonstration of the importance of including uncertainty in the decision analysis to later propose a novel methodology that employs simulation data that encapsulates both uncertainty and complexity of failures modeled by domain experts. Thus, this work is divided in two parts. The first part of this work examines how component importance measures fail to give the necessary intuition for mitigation planning in the light of uncertainty. The analysis is assisted by a novel component importance measure called *probabilistic delta centrality* that demonstrates how previously neglected stochastic considerations change decisions suggested. In the second part, a new paradigm for stochastic network mitigation is proposed. The approach leverages realizations from scenario event simulations to develop a probabilistic framework that supports constrained decision making. This scenario event simulation framework is capable of comprising component fragilities, correlation among random variables, and other physical aspects that affect component failure probabilities. On the top of that, a statistical learning model is built to enable a rapid estimation of post-disruption impact, which permits a metaheuristic to intelligently explore feasible discrete

enhancements from mitigation strategies. The search for near-optimal solutions can be restricted by limited resources and potential political, social, and safety limitations. Two examples are presented to exhibit how this method provides detailed information for mitigation. The level of complexity embedded in search along with its detailed solutions are pioneering in network mitigation planning.

Chapter 1

Introduction

Physical infrastructure networks are the backbone of modern society. Preventing large disruptions on them is associated to alleviating not only massive economic losses, but also preventing social issues (as population dislocation), and life threatening scenarios. However, the current state of these networks have serious shortfalls. For example, the American Society of Civil Engineers found 56,007 of the nation's bridges to be structurally deficient in 2016 and cite the funding necessary to rehabilitate them at $123 billion [3]. Clearly, the deteriorating physical infrastructure in the US is already susceptible to failure and even more so for certain types of natural disasters. In this context, pre-disaster mitigation analysis arises as a multidisciplinary area in which one key thrust is towards developing models of real-world physical systems and their hazard responses with a goal of providing risk-informed decision support from a systemic perspective. Decreasing the probability of failure of network components (nodes/links) via improvements/upgrades is the most frequent intervention studied because the installation of new components skyrocket costs

[4]. Thus, the focus of this work is in optimizing the way we select components in a physical network to improve, in the light of its system vulnerability to natural disasters.

Figure 1.1: Worldwide air transportation network [1]. It is an example of a network prone to costly disruptions.

Two distinct methods to address this problem are going to be foundational for this work: component importance measures and stochastic network design. In this thesis, we incorporate network failure characteristic to each of these two methods in different manners with the objective of providing more accurate and comprehensive insight for decision-making.

Network component importance measures (CIMs) quantify one or several aspects of the topology and/or functionality of the network to indirectly capture the impact of component failures. Then, components are ranked according to these values and those highly ranked are considered the most critical and, therefore, prioritized for mitigation or protection. However, in the light of uncertainty in component failures, we demonstrate that they do not provide sufficient intuition. On the other hand, the stochastic network design problem naturally incorporates uncertainty of stochastic events in networks and supports constrained optimization. Nevertheless, current solution methods based

on sampling incorporating limited complexity aspects of network failures.

This thesis proposes an approach that is able to incorporate both uncertainty and complexity network failures by extensively using external data from domain experts (based on simulation) to solve the novel formulation of the stochastic network design problem for mitigation. For this, we leverage simulation data to set up a probabilistic framework that supports constrained decision making. The network of study can be any physical network (modeled as either a directed or indirected graph) with the requirement that it should be feasible to estimate the effects between component improvement and its probability to remain present in the network after a disaster. In addition, this method does not focus on a specific performance metric as [5], but it leaves to the user the selection of a suitable performance metric for her own needs. We demonstrate the flexibility of this methodology with two examples with different networks and performance metrics.

The remainder of this thesis is organized as follows. Chapter 2 introduces the background that is foundational for this thesis. Chapter 3 develops a method to incorporate uncertainty in component importance measures, to finally conclude that they should be avoided. Chapter 4 presents the data-based methodology to incorporate complexity in mitigation planning, which is the main contribution of this work. Then, we present two examples with different settings in Chapter 5 and Chapter 6. Chapter 7 summarizes this work and its conclusions. Finally, Chapter 8 states future research work envisioned.

Chapter 2

Background

Physical networks are interconnected systems that transport goods and services whose nodes and links physically exist. Some examples of these networks are electric power networks, watter supply/sewage networks, and fiber optic networks. Due to the importance of the goods and services that these networks supply, failure on them interrupts the normal development of society (e.g. Figure 2.1) with not only economic consequences but it also deteriorates quality of life. Sabotage, human error in operation, terrorism, and natural disasters are examples of hazards that if affecting physical networks, would have different failure outcomes. For example, merely single component[1] failures are unlikely outcomes for large scale natural disasters [6, 7, 8] while this is may be a common pattern for terrorist attacks [9].

The focus of this work is in network vulnerability due to natural hazards. Natural disaster are highly impactful sporadic events that may affect a broad geographic area. Affected areas contain several networks going through them,

[1] Component is either a node or link.

Figure 2.1: Obstruction in highway.

which if some of their components get affected, it may require a major effort to recover their previous functionality. Additionally, each day that these components are not fully functional may be millions of dollars lost for the economy. Clearly, disruption of these systems should be prevented whenever is possible.

Among the four stages of the disaster cycle, i.e., mitigation, preparedness, response, and recovery [10], this thesis focuses on pre-disaster mitigation strategies. Network-specific mitigation interventions can be broadly classified in two groups: topological interventions (e.g., redundant construction, incrementing roadway capacity) and reliability-based interventions (e.g., structural retrofit, maintenance). Given the high costs of topological interventions in physical networks, reliability-based interventions are preferred.

Structural retrofit/upgrade is an example of a reliability-based intervention that provokes an increment in the likelihood to withstand a natural disaster (known as survivability probability). For example, for seismic scenarios, seis-

mic retrofit with steel jackets in columns (Figure 2.2) can shift the structure's fragility curve, which is translated to a discrete increment in the survival probability of the structure. A seismic fragility curve is a statistical tool that relates in a probabilistic manner structural damage with structural and seismic characteristics. Similar artifacts are being developed for floods and hurricanes to assess their survival probability.

Figure 2.2: Seismic retrofit for bridge using steel jackets in columns. Left: before retrofit; right: after retrofit.

For a decision-maker who wants to plan mitigation actions from a systemic perspective, the problem is about allocating resources to improve a set of components (one or more) that, by increasing their survival probability, the overall expected impact given a natural disaster would be minimal. Two methods that are capable to support decision-makers on this problem are component importance measures and stochastic network design.

2.1. Component Importance Measures (CIMs)

One common approach in network mitigation literature is based on employing component importance measures (CIMs). Methods to compute component

importance consist on measuring one or several aspects of the topology and/or functionality of the network. Once a CIM is calculated for all components, highly ranked components are recommended to be prioritized in mitigation interventions [11, 12, 13, 14].

There is a group of CIMs that share the underlying idea that the most important components are the ones whose disruption is the most impactful to an overall performance metric. We call that group *impact-based CIMs*. The CIM computation is primarily related to the choice of the network performance metric evaluated. For example, if the system metric is related to graph connectivity, an impact-based CIM would evaluate components on their ability to disconnect the network. Examples of performance metrics include network efficiency [15, 16, 17], travel demand [18], and travel time for all origin-destination nodes [9].

2.2. Stochastic Network Design (SND)

Stochastic network design (SND) is a problem setup that brings a different perspective to formulating mitigation in networks. In a stochastic network, the nodes and edges are either present or absent with certain probabilities. The probability of being present can be incremented via improvement interventions (also referred as management actions) to the component. This problem is conceived as a constrained optimization problem and falls within the category of NP-hard problems [19]. For mitigation, this problem can be re-formulated as the search for an optimal allocation strategy for available resources to reduce post-disruption impact.

Solution methods for the general form of the SND problem are based on approximate methods rooted in sampling. The most prominent one is sample average approximation (SAA) [20] that approximates the original stochastic problem to a deterministic one. For this, it employs Monte Carlo sampling from known probability distributions to identify the most frequent cases, and then solves the optimization problem for them. It disregards the least frequent cases after showing that these rare scenarios do not affect much the optimal solution. Specific methods use SAA along with intelligent search, greedy algorithms and mixed integer programming, sometimes as a two-stage stochastic optimization (e.g. [5, 21, 19]). Optimality convergence may be guaranteed for $n \to \infty$ depending on the deterministic optimization method selected [22].

2.3. Uncertainty and Complexity of Network Failures

Network failures due to natural disasters present two interconnected modeling facets: uncertainty and complexity. Uncertainty is embedded in modeling and simulating the damage state of network components in an stochastic manner, as per [23]. Damage estimation models are probabilistic artifacts to estimate probable damage patterns, which are configurations of components with an associated level of damage. Correlations and dependencies introduce complexity within component failures that affect their uncertainty. Dependencies among components from the same network and with components from other networks is considered key in modeling failure for some physical networks [24]. An example of the effect of this is the following: "Failure of A and B leads to failure

of C." On the other hand, there are correlated failures among components, which may explain more than 20% of the damage in some systems [25]. An example of the effect of this is the following: "Failure of A increases probability of failure of B."

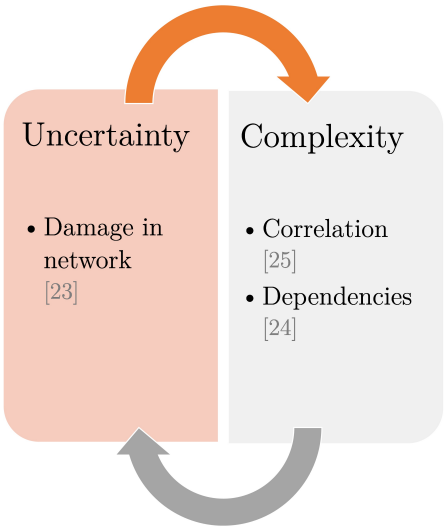

Figure 2.3: Uncertainty and complexity in network failures.

However, component importance measures and the stochastic network design problem do not fully incorporate these two aspects of network failures.

CIMs do not incorporate the uncertainty and complexity of component failures, which may prevent them to provide optimal guidance. One natural consequence of network failure uncertainty that has not been comprehensively included in CIMs is multiple component failures. Several authors using CIMs have focused their analysis in analyzing the effect of isolated failures [11, 16, 17, 26, 27, 28, 29, 30, 31, 32]. However, using this simplification may lead to misleading decisions because large synergistic effects of multiple simultaneous component failures may be overlooked [33]. For example, when comparing the loss of one major electrical substation versus the loss of two mi-

nor substations, it may be the case that the two minor ones failing represent a greater risk [34].

On the contrary, SND naturally incorporates uncertainty and there are some advances in incorporating complexity. As noted before, in disaster scenarios, independent failures are replaced by spatiotemporal correlated failures [7]. Some specific correlation has been investigated using sampling methods aided with probabilistic graphical models [35]. However, domain experts rely on other correlation methods based on experimentation (e.g. spatial correlation model for seismic ground motion [36]) that have not been included yet in SAA sampling methods. Conversely, dependencies as previously described may be incorporated in these samplers, but to the best of our knowledge they have not.

Uncertainty and complexity of network failures are captured in failure patterns, which are built by domain experts using multi-layer Monte Carlo simulations that embed results from hazard models, network estimation models, and functionality assessment. Unfortunately, SAA relies on samplers and is unable to incorporate these rich pre-defined datasets. The methodology that we propose is completely different from SAA because it comprises these datasets using machine learning to incorporate both uncertainty and complexity to the SND for mitigation. In Figure 2.4, we summarize SAA pros and cons from this perspective.

In the rest of this thesis, we incorporate uncertainty in component importance measures to show how they fail to provide sufficient insight for decision-making. Subsequently, we define the stochastic network design for mitigation and present our proposed methodology to incorporate complexity.

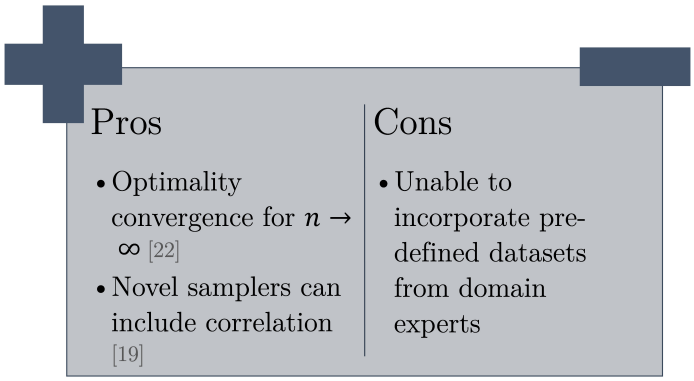

Figure 2.4: Pros and cons of using SAA

Chapter 3

Incorporating Failure Uncertainty in CIMs

In this chapter, stochastic characteristics from component failures are included in a novel CIM called probabilistic delta centrality whose strategies suggested are contrasted with the ones from impact-based CIMs.

3.1. CIM-based decision-making

3.1.1 CIM Definitions

Let $G = (\mathcal{N}, \mathcal{E})$ be the graph (directed or undirected) defined by a set of nodes $\mathcal{N}$ and a set of edges $\mathcal{E}$ that mathematically represent a network. Let $s - t$ pair be a pair of nodes so that a directed path starts from node s (source) and ends in node t (sink) such that $s \neq t$. If the graph is undirected, then there is no distinction between $s - t$ and $t - s$.

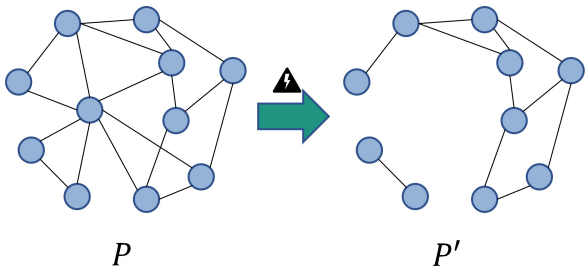

Figure 3.1: The positive drop in the performance metric after disruption is denoted as (ΔP).

Delta Centrality

In general, an impact-based CIM can be constructed from any performance metric that can be calculated in both a normal and disrupted network. Let P be a performance metric that meets this requirement. Let $(\Delta P)_i$ be defined as the drop in the performance metric when component i fails in isolation. Delta centrality [37], then, is defined in Equation (3.1).

$$C_i^{\Delta} = \frac{(\Delta P)_i}{P} \tag{3.1}$$

Network efficiency—introduced by [37]—measures how well information or goods flow in the graph as it considers the inverse of the shortest distance between each node s and t, d_{st} as shown in Equation (3.2). Its use is preferable for vulnerability analysis because it can handle infinite distances that occur in disconnected networks.

$$E = \frac{1}{N(N-1)} \sum_{s,t \in \mathcal{N} | s \neq t} \frac{1}{d_{st}} \tag{3.2}$$

Information centrality [38], denoted $C_i^{\Delta I}$, defined in Equation (3.3), is a delta

centrality based on network efficiency.

$$C_i^{\Delta I} = \frac{(\Delta E)_i}{E} \tag{3.3}$$

Note that delta centrality was proposed using a single removal strategy; thus, we refer to these as individual delta centralities. We now propose a generalized form of delta centrality.

Synergistic Delta Centrality

Definition 3.1. *Synergistic delta centrality.* Let $s_k \subseteq G$ be a set of $k > 1$ components in graph G. Let $(\Delta P)_{s_k}$ be the impact in performance metric P when all components in s_k fail simultaneously. The synergistic delta centrality for s_k is $(\Delta P)_{s_k}$ divided by the performance metric P of the network in healthy state as in Equation (3.4).

$$C_{s_k}^{\Delta} = \frac{(\Delta P)_{s_k}}{P} \tag{3.4}$$

Notationally, if $k = 2$ and $s_2 = \{i, j\}$, then let $(\Delta P)_{ij}$ denote the impact on P of the simultaneous failure of components i and j. Additionally, let C_{ij}^{Δ} denote the related synergistic delta centrality.

Similar to the individual delta centrality, a synergistic delta centrality can be defined based on network efficiency, i.e., synergistic information centrality. The synergistic delta centrality along with individual delta centralities will be used to define the probabilistic delta centrality.

3.1.2 Probabilistic Delta Centrality

A probabilistic view for the delta centrality is proposed to account for real-world aspects of component failures. This will help to pinpoint limitations of importance measures with both single and multiple removal strategies.

Definition 3.2. *Probabilistic delta centrality.* Let δ_{s_k} be a random variable associated with the impact in the performance metric P when only elements belonging to s_k fail stochastically. The probabilistic delta centrality is defined as the expected value of δ_{s_k} divided by the performance metric P of the network in healthy state, as in Equation (3.5).

$$\mathcal{C}^{\delta}_{s_k} = \frac{\mathbf{E}\big[\delta_{s_k}\big]}{P} \tag{3.5}$$

Note that δ_{s_k} takes on the value $(\Delta P)_i$ if only component i fails. Likewise, it takes the value $(\Delta P)_{ij}$ if only components i and j fail. Let p_i and p_{ij} be the probability of the isolated failure of i and probability of the simultaneous failures of i and j, respectively—the latter probability can handle correlations and failure dependencies. Then, for two components i and j, $\mathbf{E}\big[\delta_{ij}\big]$ is calculated as in Equation (3.6),

$$\mathbf{E}\big[\delta_{ij}\big] = p_i(\Delta P)_i + p_j(\Delta P)_j + p_{ij}(\Delta P)_{ij} \tag{3.6}$$

since $(\Delta P)_{\emptyset}$ is zero. By combining Equation (3.4), (3.5), and (3.6) a relationship between the probabilistic, individual and synergistic centralities is derived in Equation (3.7).

$$\mathcal{C}^{\delta}_{ij} = p_i C^{\Delta}_i + p_j C^{\Delta}_j + p_{ij} C^{\Delta}_{ij} \tag{3.7}$$

Thus, the study of component importance based on the probabilistic delta centrality can account for multiple failures and the probabilities, independent or correlated, which are associated with those failures. Similarly to the previous delta centralities, the probabilistic delta centrality for network efficiency will be referred as the probabilistic information centrality and denoted $C_{ij}^{\delta I}$.

3.2. Case Study

In this section, an example is used to demonstrate issues relating to CIMs for mitigation decision-making. The new probabilistic delta centrality provides a means to quantitatively demonstrate some pitfalls of impact-based CIMs. For this study, a geometric random graph is chosen as it resembles some critical infrastructure networks [39, 40]. The graph, depicted in Figure 3.2, has 200 nodes and 534 edges. Each of the CIMs defined in Section 3.1.1 and Section 3.1.2 are computed for the example graph.

Table 3.1 contains the top five most important components with respect to the CIM information centrality (Equation (3.3)) along with two other components that will gain importance when analyzing synergistic delta centralities.

Table 3.2 list the top five most critical two-at-a-time failures based on the synergistic information centrality. The combined failure of components 423 and 503 has the highest $C_{ij}^{\Delta I}$ value. As seen in Figure 3.2, these two components act as alternates of the other and their simultaneous failure disconnects the graph.

Table 3.2 reveals an interesting facet of multiple failures. However, it may be that the combination of components with the highest synergistic centrality

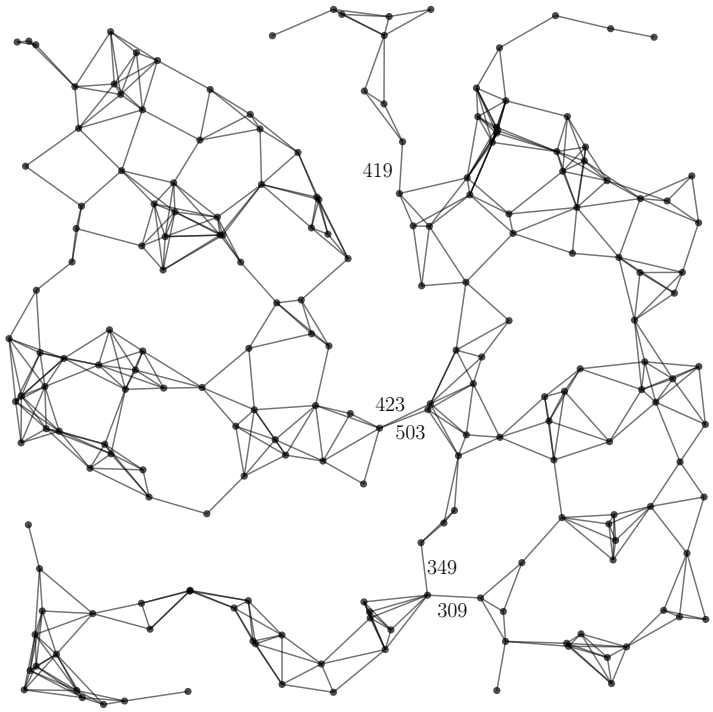

Figure 3.2: Random geometric graph of 200 nodes and 534 edges. Selected edge indexes are labeled.

has a very low probability of simultaneous failure. This would be potentially misleading for mitigation decision-making. The probabilistic delta centrality can be used to demonstrate how failure probabilities can affect ranking and thus mitigation decision-making.

3.2.1 Analysis with the Probabilistic Delta Centrality

Consider a simplistic example, based on the topology shown in Figure 3.2, in which each of the components fail independently and with the same probability p. Hence, for two components, the probability of exactly one failure is $p(1-p)$,

Table 3.1: Top five components along with two other components that serve in the discussion.

$i \in \mathcal{E}$	$C_i^{\Delta I}$
419	0.0536
349	0.0206
112	0.0180
309	0.0169
325	0.0169
423	0.0013
503	0.0013

Table 3.2: Top five synergistic information centralities for combinations of two edges.

$\{i, j\}$	$C_{ij}^{\Delta I}$
{423, 503}	0.2609
{309, 349}	0.1471
{349, 419}	0.0736
{112, 419}	0.0707
{309, 419}	0.0706

while the probability of simultaneous failures is p^2. The probabilistic delta centrality $\mathcal{C}_{ij}^{\delta}$ for two components $i, j \in G$ becomes a function of a single probability and simplifies to Equation (3.8):

$$\mathcal{C}_{ij}^{\delta} = p(1-p)\left(C_i^{\Delta} + C_j^{\Delta}\right) + p^2 C_{ij}^{\Delta} \tag{3.8}$$

In the given example, if a decision is to be made to improve or protect exactly two components (e.g., due to a limited budget, etc.) using information centrality as the system performance metric, the pair of components that should be selected changes with respect to the value of p.

For $0 < p \leq 0.55$, the highest value for $\mathcal{C}_{ij}^{\delta I}$ is for the component set $\{309, 349\}$

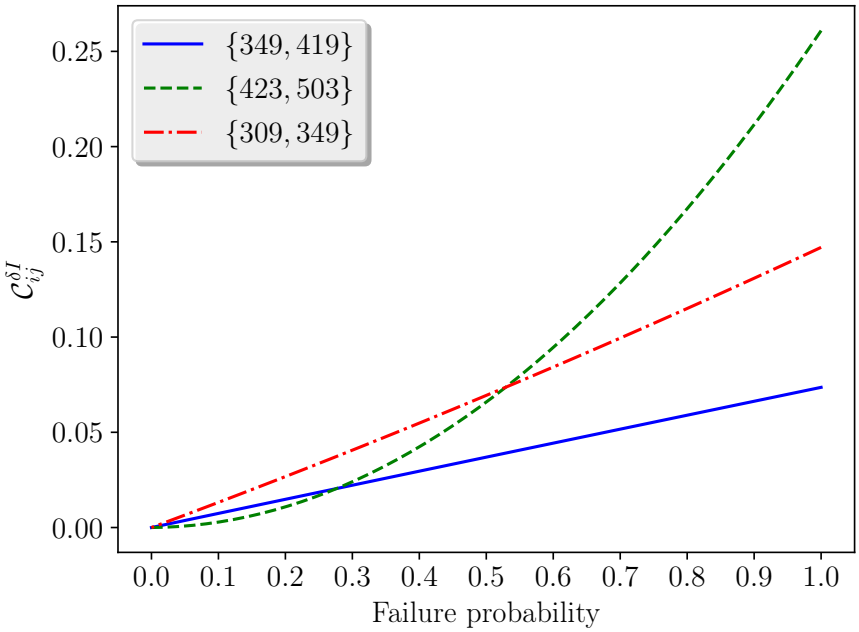

Figure 3.3: Probabilistic information centrality as a function of failure probability p for select pairs of components.

(Figure 3.3). This combination is second in importance with respect to the synergistic information centrality. The probability of both components 309 and 349 failing simultaneously is less than 0.3025. For higher failure probabilities, $p > 0.55$, the set $\{423, 503\}$ is the best selection. This agrees with the top ranked pair in Table 3.2. In general, the probabilistic delta centralities, under the highly unlikely assumption of independent and equal failure probabilities with $p = 1$, is equivalent to the implied assumptions and results for synergistic delta centralities.

The values for probabilistic information centralities of the top three pairs of components from Table 3.2, i.e., $\{423, 503\}, \{309, 349\}$, and $\{349, 419\}$, are plotted in Figure 3.3. The third ranked pair of important components in Table 3.2, which are also the top two components based on a ranking of the individual

information centralities (Table 3.1), are never the optimal mitigation choice across all values of p. Clearly, synergistic delta centrality captures only one aspect of the full spectrum of analysis possible with the probabilistic delta centrality approach.

The simplifications related to independent and equal failure probabilities are not necessary with the probabilistic centrality measures. Realistic failure probabilities as induced by various hazards (e.g., the probabilities of damage states associated with an earthquake of a given magnitude) are easily incorporated in the calculations.

Note that the probabilistic delta centrality requires the calculation of all synergistic delta centralities which may be very costly depending on size of the network and performance metric selected. For example, for this random graph with 200 nodes, it took about one week to calculate the synergistic delta centrality for $k = 2$ distributed in 30 parallel threads in a 2.4 GHz server. If we had $k > 2$, the number of combinations to evaluate would increase exponentially. Therefore, in practice, its use is limited by this computational considerations.

3.3. Concluding Remarks

Network component importance measures for mitigation decision-making using may provide misleading guidance. This is indicated with the analysis driven by the probabilistic delta centrality, a novel CIM which accounts for probabilities of component failures. Unfortunately, the computational limitations of the probabilistic delta centrality are an obstacle. Nevertheless, the empirical

results from its use shed light on desirable characteristics for component-level mitigation decision support. Any pre-disaster ranking which does not adequately address uncertainty has limited decision support value. Even under the simplifying assumption that all elements fail independently and with equal probability, the previous example has shown that they may not follow deterministic rankings.

There are other limitations for CIMs. They are completely independent of external economic constraints and others that may prevent improvement in certain components like social, political and safety limitations. The inclusion of these limitations would not longer guarantee that highly ranked components should be prioritized for mitigation. In addition, this method cannot handle the discrete levels of improvement that some component networks may presented as noted in Chapter 2. Due to all these reasons, we recommend to exclude CIMs as a possibility for stochastic mitigation.

Chapter 4

Incorporating Failure Complexity in SND

The interdisciplinary nature of hazard mitigation planning requires decision frameworks to be easily adapted to the input from simulations developed by domain experts (e.g. geologist, hydrologist, civil engineers). The common ground for these experts is Monte Carlo simulation. Several layers of Monte Carlo simulations (from hazard simulation to network damage estimation) outputs a dataset of probable failure patterns for the network. This dataset encapsulates a high amount of complexity modeled by a diverse set of experts. Thus, a compelling decision support tool should take advantage of the availability of these models and provide guidance with respect to realistic system constraints. However, current solution approaches for the stochastic network design (SND) problem do not benefit from these advances. In this chapter, we propose a way to include this rich dataset in solving this kind of problems.

4.1. Adapting SND to Mitigation

In the general SND problem, networks present stochastic characteristics in diverse ways. For example, nodes/links can be present or absent with a probability, or link capacities, weights or lengths may take discrete or continuous values in a stochastic way, which may represent the traffic status for a given hour of the day. Management actions can change these probabilities. SND includes the costs linked to actions to search for a suitable management strategy. This general problem can be formulated for network mitigation in the following manner.

Let $G = (\mathcal{N}, \mathcal{E})$ be the a graph (directed or undirected) defined by a set of nodes $\mathcal{N}$ and a set of edges $\mathcal{E} \subseteq \mathcal{N} \times \mathcal{N}$ that mathematically represent a network. The network components (including both nodes and edges) are indexed from 1 to N. Assume the state of any component as being either functional (survived) or non-functional (failed) after a disruptive event. Let p_i be the *survival probability* [21], which is the probability of the component i to survive and can be determined by structural analysis [41]. Conversely, $1 - p_i$ denote the probability of failure for component i. Let $\mathbf{p} = \langle p_1, \cdots, p_N \rangle$ be the representation of the current state of the network component's survival probabilities.

Realistically, a component's survival probability value can not be improved to *any* level (improvement in survival probabilities is not continuous as explained in Chapter 2). As such, we assume that a component's survival probability can be improved according to a finite set of discrete values (e.g., a building might be retrofit to a higher code level resulting in a specific shift in the structure's fragility curve). Each survival probability increment is associated

with a list of possible *levels of improvement* according to available mitigation interventions. For example, a building with survival probability 0.90 may have three levels of improvement (0.93, 0.95, and 0.97) based on retrofits associated with enhanced building codes. Each level of improvement has a cost associated with labor, materials, and other required resources. Furthermore, we realize that for decision-makers there may be other concerns besides finances such political, social, or safety limitations that prevent interventions for certain components.

Among the constraints that this problem considers are the following. It may be that due to social, political, safety or other issue it is not possible to improve one component or a combinations of components. There may be constraints on the number of components to be improved imposed by external regulations. Additionally, budgetary or resource limitations need to be addressed.

The problem objective relates to the expected value of a post-disruption performance metric φ that is aligned with a desirable outcome for G. Many performance metrics exist in the literature relating to various infrastructures, e.g., travel time in transportation systems [42], expected cost of direct hazard damage [43], commodity flow [11], among others. The decision variable is the vector $\mathbf{x}$ that represents the discrete improvements to be performed in the network having $\mathbf{p}$ as baseline.

In summary, the problem addressed is to minimize post-disruption impact on φ by choosing network components for mitigation interventions that improve their survival probabilities for a given hazard subject to limited financial resources and other political, social, and/or safety standards that impose constraints on component selection.

4.2. Data-based Stochastic Network Mitigation

Our proposed methodology called *data-based stochastic network mitigation* is completely different from the sample average approximation (SAA) introduced in Section 2.2. The approach ingests data from Monte Carlo simulations to build up a probabilistic framework that supports constrained optimization. This constrained optimization is driven by a metaheuristic search whose objective is to look for near-optimal values of performance metric φ. This process is facilitated by a statistical learning model that relates φ with survival probabilities associated with improvement strategies. Therefore, a probabilistic representation of the simulation dataset is required for the construction of this statistical learning model.

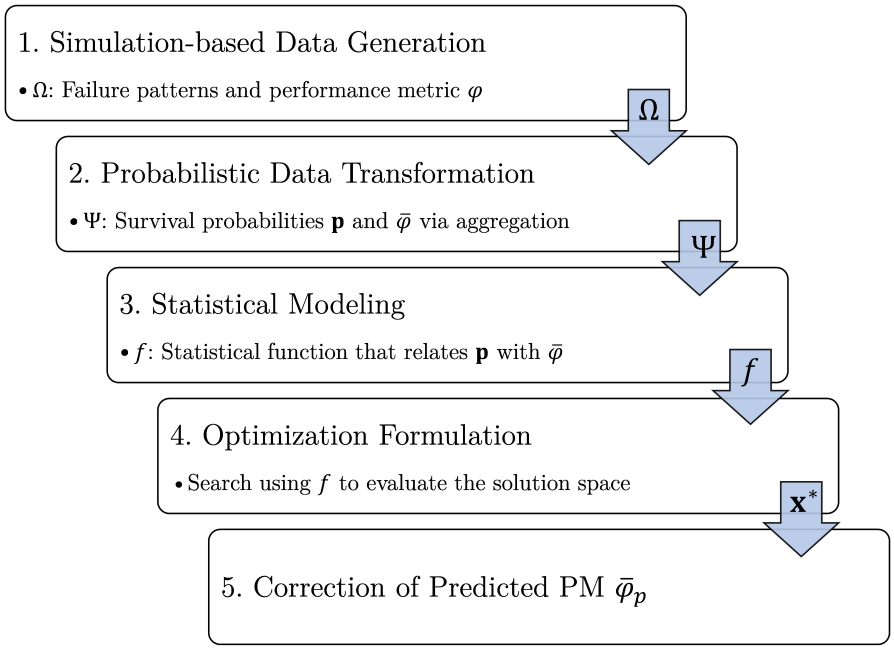

Figure 4.1: Overview of the proposed methodology.

This methodology has three steps to build the statistical learning model (Sec-

tions 4.2.1, 4.2.2, 4.2.3). Then, it uses the regression model to find near-optimal solutions in a constrained optimization framework (Section 4.2.4), and finally correct these solutions (Section 4.2.5). These steps are depicted in Figure 4.1.

4.2.1 Simulation-based data generation

The simulation data should be based on hazard specific and component specific fragility curves. A fragility curve depicts the probability of a component exceeding a given damage state as a function of hazard intensity. Once a hazard intensity is selected for analysis, Monte Carlo simulations and damage estimator models are used to estimate the impact to system components. Oftentimes, the damage states include multiple discrete levels (e.g., slight, moderate, extensive, complete), but converting to a binary representation (functional and non-functional) is straightforward, and arguably appropriate for failures caused by a disaster [44]. The results from the collection of Monte Carlo realizations provide a rich set of data that represent likely failure patterns.

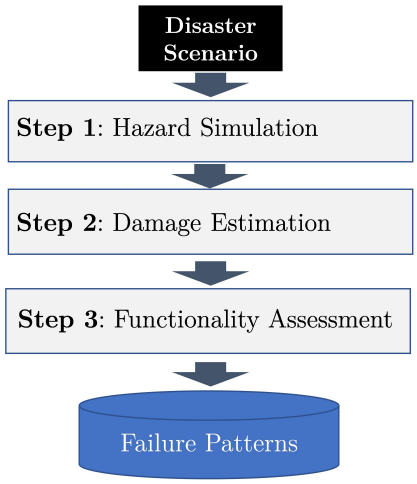

Figure 4.2: Multi-layer Monte Carlo Simulation (MCS).

Finally, for each of the simulation realizations, the network performance metric φ is computed. We refer to the combination of plausible failure patterns and the associated performance metric evaluations as a subset of the *realization space* and denote the dataset as Ω containing n observations. If the network contains N components, then an example excerpt of Ω could look like Table 4.1, where a value of 1 denotes that a component is functional (survived) and a value of 0 denotes that a component has failed. The data in Ω is used to estimate a *probabilistic space* which incorporates expected values of the performance metric. The average of each column from this dataset (from 1 to N) is designated as the baseline state for the network survival probabilities.

Table 4.1: Example observations in realization dataset Ω.

Realization	Component 1	Component 2	$\cdots$	Component N	φ
1	1	1	$\cdots$	0	13.32
2	0	1	$\cdots$	1	14.81
$\vdots$	$\vdots$	$\vdots$	$\vdots$	$\vdots$	$\vdots$
n	1	0	$\cdots$	1	12.74

4.2.2 Probabilistic data transformation

A subset of the *probabilistic space* is denoted as Ψ, and it relates components survival probabilities with expected values of the performance metric. This is accomplished by sampling with replacement[1] η rows from Ω. The component statuses and φ values from each of the η samples are averaged together to create a dataset Ψ with m observations and $N+1$ values. Thus, each observation in Ψ is a vector of survival probabilities $\mathbf{p}$ and an average of the performance metric

[1]Sampling with replacement allows to cover more values in the probabilistic space.

that is denoted as $\bar{\varphi}$. An example of this dataset is illustrated in Table 4.2.

Table 4.2: Example observations in probabilistic dataset Ψ.

Prob. Sample	Component 1	Component 2	$\cdots$	Component N	$\bar{\varphi}$
1	0.68	0.88	$\cdots$	0.96	12.62
2	0.72	0.92	$\cdots$	0.76	12.92
$\vdots$	$\vdots$	$\vdots$	$\vdots$	$\vdots$	$\vdots$
m	0.88	0.8	$\cdots$	0.84	13.22

The selection of the sample size η needs some reflection because it affects the accuracy of the statistical model in two conflicting ways. First, η affects the accuracy of the expected performance metric $\bar{\varphi}$: the higher η is, the more accurate $\bar{\varphi}$ is (law of large numbers). Second, η governs the number of probabilistic samples that are going to fall within the prediction boundaries for the statistical model (i.e. where this model is going to be predicting when used for optimization). Each of the columns of the probabilistic dataset follow a Binomial sample proportion distribution which approximates to a normal distribution with mean equals to p_i and variance of $p_i(1-p_i)/\eta$. Therefore, if η increases, σ shrinks, which means that by increasing η, some parts within the prediction boundaries may have fewer examples, which is undesirable to train the statistical model as it may compromise the accuracy of the predictions within these boundaries. Thus, the selection of η needs to consider the tradeoffs between accuracy of $\bar{\varphi}$, and accuracy of the statistical model in the optimization framework.

The following considerations can be taken to suggest a way to handle this tradeoff. As noted before, the survival probabilities in Ψ for each component follow approximately a normal distribution with mean p_i (baseline survival

probability for component i). The lower boundary of prediction is always going to p_i, and the upper boundary depends on the probabilities associated with the feasible levels of improvements. The difference between the upper and lower boundary for a component i is called the range of prediction (denoted as R_i), which can be viewed as a deviation from the mean. Thanks to this, a relationship between R_i and σ_i can be formulated in Equation (4.1) so that most data is going to fall within the range of prediction. The standard deviation is multiplied by 2 to ensure the tail of the Gaussian within the boundaries is not too thin, i.e. not many observations near the upper boundary.

$$R_i \leq 2 \cdot \sigma_i \approx 2 \cdot \sqrt{p_i(1-p_i)/\eta} \tag{4.1}$$

4.2.3 Statistical modeling

Statistical learning methods, especially non-linear machine learning models, are designed to fit the complex relationships between inputs and outputs embedded in the probabilistic data Ψ. We employ such methods to derive f as an estimate of the relationship between $\bar{\mathbf{p}}$ and $\bar{\varphi}$, i.e., $\bar{\varphi} \approx f(\mathbf{p}) = \bar{\varphi}_p$, where $\bar{\varphi}_p$ is the predicted average performance value to be optimized.

The focus on building a machine learning model for this methodology is on predictability. We want this model to be able to predict the expected performance metric for an improvement strategy that we want to evaluate because these predictions will be used to evaluate how good a feasible solution is. Thus, it is recommendable to try models with high predictability as boosted and ensemble methods, deep neural networks, and others.

4.2.4 Optimization formulation

The mathematical formulation of this problem follows:

$$\text{max (or min)} \quad \bar{\varphi}_p \tag{4.2}$$

$$\text{s.t.} \quad cost(\mathbf{x}) \leq \text{Budget} \tag{4.3}$$

$$x_i \leq l_i \qquad \forall i \in \{1, \cdots, N\} \tag{4.4}$$

$$z_i = \begin{cases} 1, \ x_i > 0 \\ 0, \ x_i = 0 \end{cases} \qquad \forall i \in \{1, \cdots, N\} \tag{4.5}$$

$$\sum_{i=1}^{N} z_i \leq k \tag{4.6}$$

$$x_i \in \mathbb{Z}_{\geq 0} \quad \wedge \quad z_i \in \{0, 1\} \qquad \forall i \in \{1, \cdots, N\} \tag{4.7}$$

The decision variable $\mathbf{x} = \langle x_1, \cdots, x_N \rangle$ are integers denoting the improvement options for each component, where for example, $x_1 = 0$ implies that component 1 should be left at its baseline state of p_1, whereas $x_1 = v$ implies that component 1 should be retrofit to level $v > 0$ which will result in a higher survival probability than the baseline. The function $cost(\mathbf{x})$ relates discrete survival probability improvements with their intervention costs. The parameter l_i is the maximum level of improvement for component i; z_i is a binary variable that takes on a value of 1 if component i is selected and 0, otherwise; and $k \leq N$ is the total number of components available for enhancement.

Constraint (4.3) represents the economic limitations. Constraint (4.4) fixes the maximum level of improvement for each component. If mitigation efforts are not feasible for component i (due to physical, political, or other reasons) l_i is

set to zero. Constraint (4.5) relates x_i and z_i. Constraint (4.6) sets a limitation on the number of components that can be enhanced. Constraint (4.7) sets the domain for the decision variables.

The solution method for this optimization problem depends on the selected statistical model and the function $cost(\mathbf{x})$. If $cost(\mathbf{x})$ is linear or easy to linearize, it may be worth trying a linear regression model because it would allow us to use a MIP (mixed-integer programming) solver and guarantee getting to the global optima. On the other hand, having non-linear relationships in our optimization formulation may required approaches as metaheuristic search, which provide local optima solutions. In the latter case, as metaheuristic approaches are stochastic methods, the search should be repeated with different seeds to find several different solutions from which the best one should be chosen. Whether the solutions are global or local optima, they will be represented as $\mathbf{x}^*$ in the rest of the thesis.

4.2.5 Correction of expected performance metric value

The objective value $\bar{\varphi}_p$ of the solution(s) obtained in the previous step are predicted values of the expected performance metric. There are two sources of error for this estimate: the sampling error known as standard error of the mean (Section 4.2.2), and the error of the statistical model (Section 4.2.3). The standard error of the mean is estimated with Equation (4.8).

$$\sigma_{\bar{\varphi}} \approx s/\sqrt{\eta} \tag{4.8}$$

where s is the standard deviation of the performance metric in the realization

dataset, and η is the sample size calculated in Section 4.2.2. On the other hand, the error of the statistical model can be estimated from the square root of the mean squared error of the model predicting in the test set. Therefore, these $\bar{\varphi}_p$ are inaccurate estimates, however, they are useful for exploring the solution space. Once solutions $\mathbf{x}^*$ have been identified, the inaccurate estimate for its performance metric can be corrected in the following manner.

A new realization dataset similar to Ω with size n' can be generated by simulating the system with the new survival probabilities obtained from the solution $\mathbf{x}^*$. Then, $\frac{1}{n'}\sum_{i=1}^{n'}\varphi$, which converges to the actual expected performance metric as n' goes to infinity (law of large numbers), can be a better estimated of the expected performance metric given the selected improvements. This value will be denoted as $\bar{\varphi}_c$.

To select a value for the sample size n', we suggest the following procedure based on confidence intervals.

1. Calculate the performance metric φ for a set of $m \in \mathbb{N}$ failure patterns generated using probabilities associated with solution $\mathbf{x}^*$.

2. Calculate the performance metric mean $\bar{\varphi}_m$ and standard deviation s_m. The sub-index m represents that these point estimates were calculated with the initial m samples.

3. Select a desired level of error ϵ (multiplied by $\bar{\varphi}$ results in the margin of error) and a significance level α for that margin of error.

4. Use Equation (4.9) to get a lower bound for n' where $Z_{1-(\alpha/2)}$ is the z-score of the standard normal distribution. Use student-t-distribution rather than the normal distribution for $m < 30$.

$$n' \geq \left(\frac{Z_{1-(\alpha/2)} \cdot s_m}{\epsilon \cdot \bar{\varphi}_m} \right)^2 \tag{4.9}$$

Chapter 5

Example 1: Shelby County Transportation Network

5.1. Scenario Setup

The network topology from Shelby County, Tennessee is utilized to demonstrate an application of the proposed methodology for a seismic event. Shelby County is located in the southwest part of the state of Tennessee, and contains the city of Memphis, which is the second-largest metropolitan area in Tennessee.

Figure 5.1 shows a simplified Shelby transportation network in which only major highways and their bridges are depicted. The components considered vulnerable to an earthquake hazard for this study are the 24 bridges portrayed in the figure, i.e. $N = 24$. The nodes are either intersections of major highways or intersections of a highway with the limits of the county.

For a given earthquake hazard, the reliabilities of the bridges are known, yet for

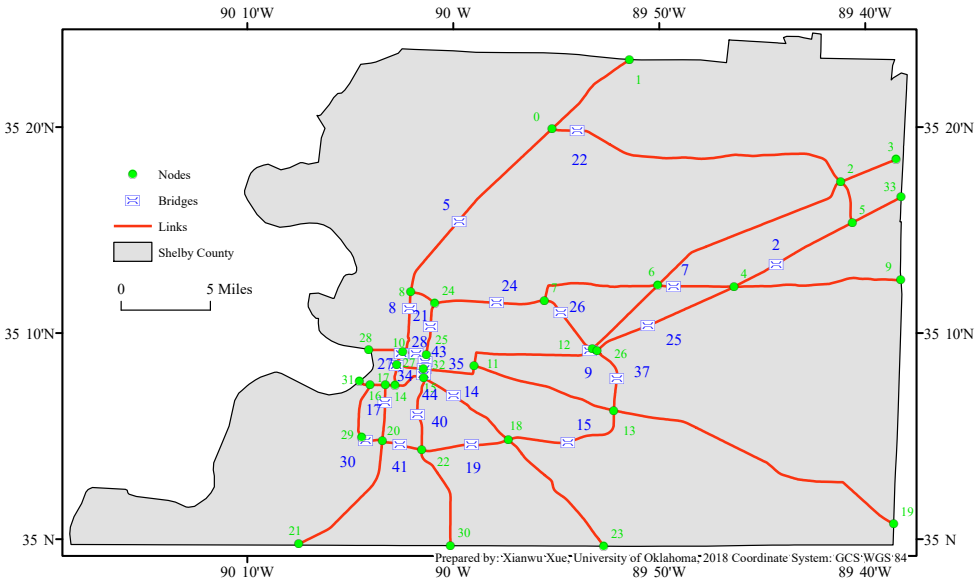

Figure 5.1: Shelby County transportation network, only major highways depicted

demonstration purposes are assumed to be equal at 0.8. Further assumptions are that each bridge can be improved up to four different levels of reliability (0.85, 0.9, 0.95, and 0.97) and the associated costs are known ($100,000, $220,000, $300,000, and $360,000). The objective is to maximize the post-disaster performance network efficiency.

Four constraint cases for long-term mitigation are studied separately. They are motivated by real-world limitations and selected to use the mathematical constraints described in 4.2.4.

Case 1 Select at most three bridges to improve with unlimited budget.

Case 2 Budget available of $500,000.

Case 3 Budget available of $1,500,000.

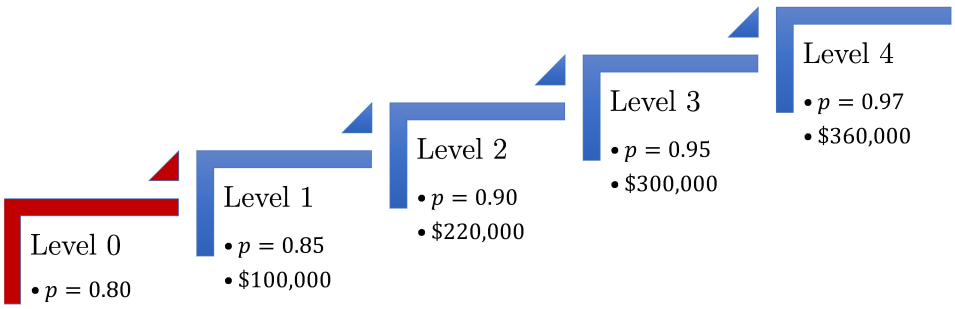

Figure 5.2: Levels of improvement with associated survival probabilities and costs.

Case 4 Two bridges with the highest delta centrality (44 and 35) can not be improved due to social/political reasons. Budget available of $1,500,000.

5.2. Application of Methodology

5.2.1 Data Generation and Transformation

The failure data for each component is generated via Monte Carlo simulation using independent Bernoulli trials with probability of success equal to 0.8. Once the whole dataset is generated, the network efficiency (Equation (3.2) is calculated for each network failure pattern.

For this example, the prediction boundaries for all components are 0.8 as lower boundary and 0.97 as upper boundary (within these boundaries the statistical model is going to predict). Let us apply Equation (4.1) to have an upper

bound for η.

$$0.97 - 0.80 \leq 2 \cdot \sqrt{0.8 \cdot 0.2/\eta}$$

$$\eta \leq 22.15$$

Then, we select a round number for η that is below 22.15: $\eta = 20$. A less precise way to select η is visually by plotting histograms of the survival probabilities of each component for different values of η. Figure 5.3 shows that the histogram for $\eta = 20$ is more suitable than its counterpart with $\eta = 40$ because the Gaussian tail is thicker for values around 0.95, which will help the learning algorithm to make better predictions for those probability values.

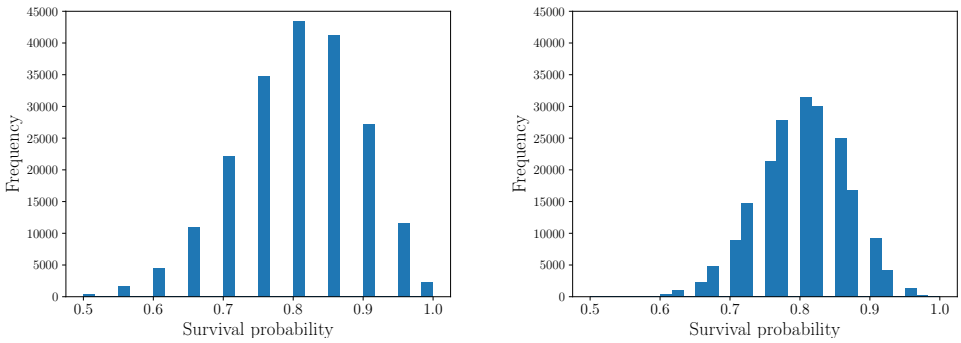

Figure 5.3: Histograms of component survival probabilities. Left, sampled with $\eta = 20$; right, sampled with $\eta = 40$.

5.2.2 Statistical Modeling

A random forest is used as the statistical learning model to learn the complex relationships embedded in the probabilistic dataset. First, this probabilistic dataset (20,000 observations) is divided in two: train set (80%) and test set (20%). To select appropriate parameters for this random forest model, a

cross-validation with $k = 5$ is performed within the train set with the hyper-parameter grid described in Table 5.1.

Table 5.1: Hyper-parameter values considered in tunning the random forest. Selected in bold.

Hyper-parameter	Values
No. of estimators	200, 400, 600, 800, 1000, 1200, 1400, 1600, **1800**, 2000
Maximum depth	10, 20, 30, 40, 50, 60, 70, 80, 90, **100**, None
Max. features on split	$\mathbf{N}, \sqrt{N}$

In Table 5.1, the number of estimators is the number of trees that are going to be part of the ensemble. The maximum depth controls the depth of each tree in the ensemble. The maximum number of features on split is the number of features that will be considered in each split. In the case of the N option, it considers all the features for split. In the case of the $\sqrt{N}$ option, it considers a number of features equal to the square root of the total number of features. The metric used to tune these hyper-parameters is the mean squared error (MSE).

With the tuned hyper-parameters (shown in bold in Table 5.1), a learning curve (Figure 5.4) is built running 5-fold cross-validation repeatedly for several training set sizes. It can be noted in Figure 5.4 that the current random forest model has a low training error compared with the validation error, which is a sign of overfitting. In this cases, it is recommended to reduce the complexity of the model using regularization. For this specific random forest, the parameter maximum observation per leaf node is selected as a regularization parameter. After experimenting with several values for this parameter, we select to set it to be 200 (based on its validation error). The learning curves after this regularization are now closer, which suggests that the new model is less biased

and apt for better generalization.

In addition, from this learning curve, it can be noted that a size of 2,500 is necessary to avoid overestimation of the validation error. This result tell us two things: (1) using 2,500 samples for training in cross-validation should be ensured to get a proper error estimation for tuning; (2) to meet the requirement in (1) with 5-fold cross validation, it is needed to have at least $2,500 \times 5/4 = 3125$ samples for training. Therefore, we do not need to use the 16,000 samples that were initially generated by the probabilistic transformation.

The final model was build with the parameters from the cross-validation and regularization. Its performance metrics mean squared error (MSE) and mean absolute error (MAE) were 2.32×10^{-6} and 0.0012 respectively. To have other assessment of the quality of the model, we made a reliability curve for the test set shown in Figure 5.5, where the closest the red line is to the gray dashed, the lower the bias error. This curve answers the question: "Given a predicted average $\bar{\varphi}_p$, what is the most likely observation of the actual $\bar{\varphi}$?" It can be noted that the lower extreme has high bias error, therefore, it should be expected that those those values the prediction is overestimating the actual average performance metric. In contrast, the other end of the graph seems to have a low bias.

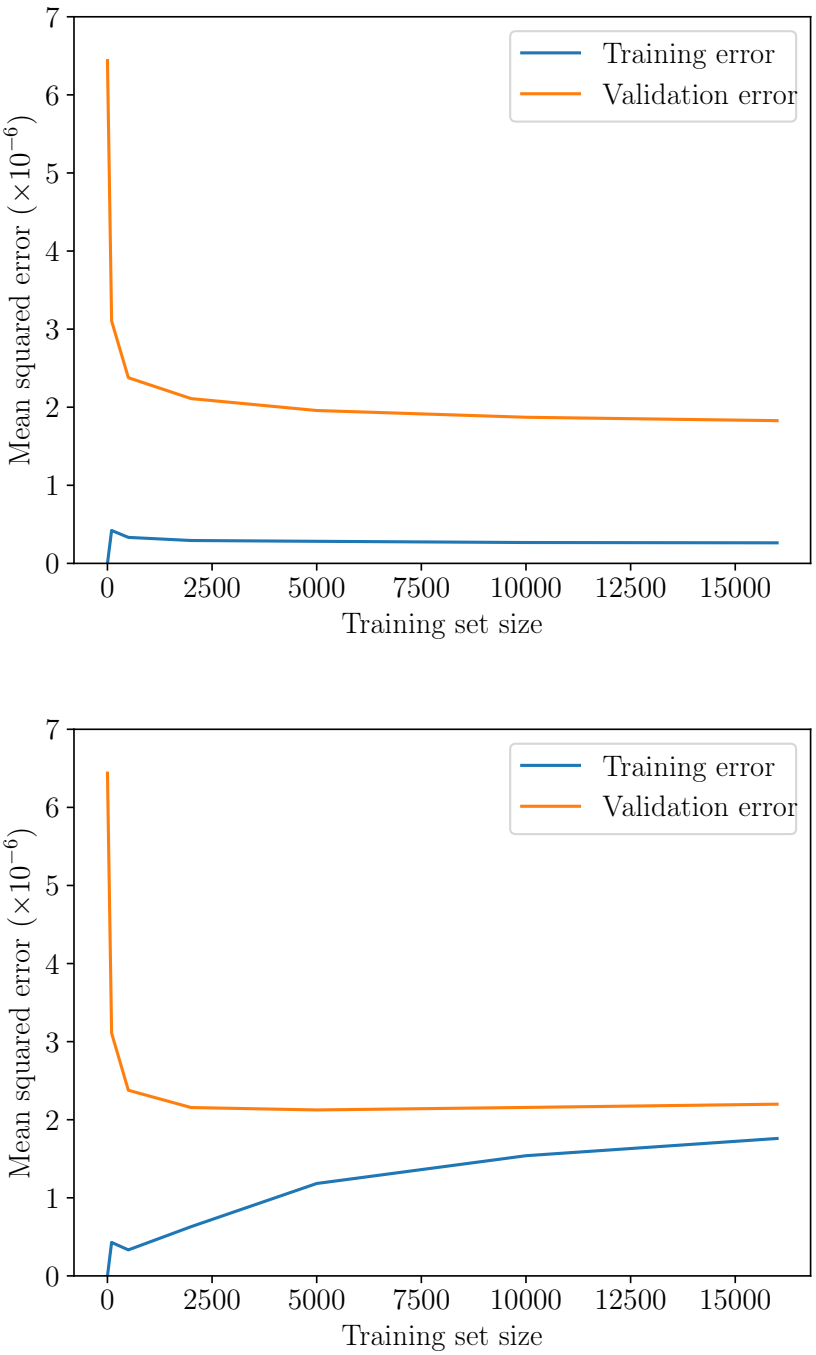

Figure 5.4: Learning curve for random forest model before (above) and after (below) regularization.

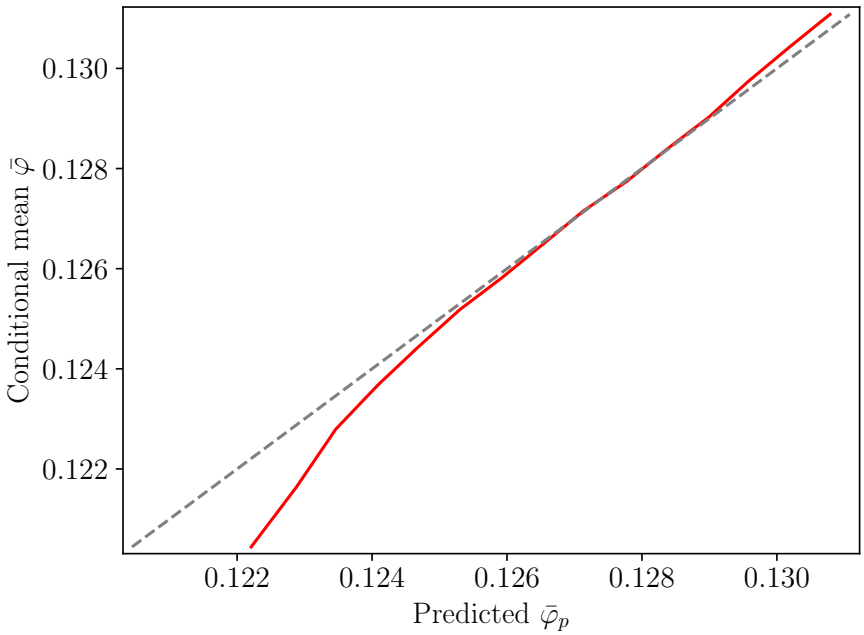

Figure 5.5: Reliability curve for final random forest model. Gray dashed line is a perfect reliability curve. Red is actual.

5.2.3 Optimization

A genetic algorithm is used to explore the probabilistic solution space using the previous machine learning model to estimate the expected value of the performance metric for each improvement strategy. The selected parameters are presented in Table 5.2.

Table 5.2: Genetic algorithm parameters.

Parameter	Value
Cross-over probability	0.5
Mutation probability	0.2
No. of Generations	500
Population Size	800

In Table 5.2, the cross-over probability is the likelihood of two parent solutions to be combined to get new children solutions; otherwise, they will not change. This probability is suggested to be set to 0.5 [45]. The mutation probability is associated to changing one of the chromosomes of children solutions. The number of generations sets how many times old population are going to perish to give birth to new ones. Finally, the population size is the number of individuals (solutions) in each generation. The last three parameters are set via empirical analysis.

In order to run the genetic algorithm with the selected parameters, the constraints must be defined. Each constrain case is related to a mathematical constraint introduced in Section 4.2.4 in the following manner.

Case 1 Set $k = 3$ in Constraint (4.6)

Case 2 Set Budget $= \$500,000$ in Constraint (4.3)

Case 3 Set Budget = $\$1,500,000$ in Constraint (4.3)

Case 4 Set $l_i = 0$ for bridges 44 and 55 in Constraint (4.4) and set Budget = $\$1,500,000$ in Constraint (4.3)

Note that the function $cost(\mathbf{x})$ from Constraint (4.3) is non-linear for this problem, thus, it can be coded as a look-up table.

Metaheuristic approaches are stochastic methods, therefore, the search for solution for each constraint case should be repeated with different random seeds to find several different solutions from which the best one should be chosen. The corrected estimates of performance metric for each of these solutions should be compared to select a final solution for each case.

5.2.4 Correction of Predicted Performance Metric $\hat{\varphi}_p$

In Equation (4.9), $Z_{1-(\alpha/2)}$ for level of significance $\alpha = 0.05$ will take $Z_{0.975} = 1.96$. Then, we decide to have a level of error of $\epsilon = 1\%$. Taking $m = 1000$, we can calculate the average performance metric $\bar{\varphi}_m$ and the standard deviation for the performance metric s_m for each of the solutions. The following is an extract of the best solutions for each constraint case. Remind that for each constraint case there were several runs of the genetic algorithm to ensure get several local optima. Each of these local optima has to be corrected.

Case 1 $\bar{\varphi}_m = 0.1325$ and $s_m = 0.0067$ result in $n' \geq 98.22$

Case 2 $\bar{\varphi}_m = 0.1305$ and $s_m = 0.0083$ result in $n' \geq 155.40$

Case 3 $\bar{\varphi}_m = 0.1337$ and $s_m = 0.0056$ result in $n' \geq 67.39$

Case 4 $\bar{\varphi}_m = 0.1327$ and $s_m = 0.0061$ result in $n' \geq 81.18$

Looking at the lower bounds for n' for each constraint case, it is clear that the average performance metric calculated with 1,000 samples fulfills the significance level and level of error required. Therefore, the calculated values for $\bar{\varphi}_m$ can be used as the corrected performance metric $\hat{\varphi}_p$, which are presented in Table 5.3.

5.3. Results and Discussion

The solutions $\mathbf{x}$ are presented in Table 5.3 for each of the four cases described. The solutions from the proposed approach are compared to a CIM ranking based approach using the individual information centrality $C_i^{\Delta I}$ introduced in Section 3.1.1.

From Table 5.3, a key finding is that the CIM-ranking has a mixed and even poor relationship with the best solutions for a decision maker. In Case 1, when three bridges are desired, bridge 34, ranked third according to the CIM, is not chosen to be improved. In Case 2, with a restrictive budget, the priority is on bridges ranked fourth and fifth rather than bridges ranked second or third. In Case 3, when the budget increases to \$1,500,000, five bridges are chosen from the top five CIM ranked positions, however, the level of improvement is does not correspond perfectly to their CIM ranking. In the final case in which the two bridges with the highest information centrality values are removed from consideration, the CIM ranking would fail to recognize the importance of bridges 21, and 14 – all ranked relatively low according to the $C_i^{\Delta I}$ value.

For three of the cases presented, the absolute difference between $\bar{\varphi}_p$ and the $\bar{\varphi}_c$ is higher than the expected MAE (0.0012). The reason for this is the following. The MAE is calculated only for the regression model, and the error in $\bar{\varphi}_p$ comes from two sources: sampling error (0.0014 calculated using Equation (4.8)) and the statistical model error (0.0015). Hence, it should not be a surprise to have this difference out of the MAE range. It is worth reporting that from our experiments with different seeds for the genetic algorithm and correcting several different solutions for each case, it is noticed that the estimates of $\bar{\varphi}_p$ for this problem presented a strong correlation with $\bar{\varphi}_c$, which provides support to say that the statistical model is useful for exploring the solution space.

Table 5.3: Solutions for constrained cases with bridge indexes sorted by information centrality $C_i^{\Delta I}$. Each solution column contains the level of improvement suggested for each component i, from 0 (no improvement) to 4 (highest improvement). At the bottom, predicted average performance metric $\bar{\varphi}_p$ (objective) and corrected expected performance metric $\bar{\varphi}_c$ for each solution.

Bridge ID	CIM	Solution $\mathbf{x}^{*(j)}$ to constraint case j			
i	$C_i^{\Delta I}$	$x_i^{*(1)}$	$x_i^{*(2)}$	$x_i^{*(3)}$	$x_i^{*(4)}$
44	0.0537	**4**	**3**	**3**	-
35	0.0380	**4**	0	**3**	-
34	0.0346	0	0	**3**	**4**
27	0.0328	**4**	**1**	**2**	**3**
43	0.0292	0	**1**	**4**	**4**
30	0.0156	0	0	0	0
41	0.0154	0	0	0	**4**
5	0.0149	0	0	0	0
24	0.0125	0	0	0	0
28	0.0124	0	0	0	0
37	0.0120	0	0	0	0
21	0.0116	0	0	0	**1**
9	0.0104	0	0	0	0
17	0.0082	0	0	0	0
26	0.0078	0	0	0	0
2	0.0077	0	0	0	0
14	0.0077	0	0	0	**1**
40	0.0067	0	0	0	0
19	0.0064	0	0	0	0
8	0.0062	0	0	0	0
15	0.0057	0	0	0	0
7	0.0043	0	0	0	0
22	0.0028	0	0	0	0
25	0.0018	0	0	0	0
$\bar{\varphi}_p$ (predicted)		0.1306	0.1301	0.1312	0.1304
$\bar{\varphi}_c$ (corrected)		0.1325	0.1305	0.1337	0.1327
Thous. of USD spent		1,080	500	1,480	1,480

Chapter 6

Example 2: IEEE 30-bus Test System

6.1. Scenario Setup

The IEEE 30-bus test system [46] (Figure 6.1) depicts a portion of the U.S. Electric Power System and is utilized as an example where vulnerable components are both nodes and links, with different survival probabilities and levels of improvements. The graph simplification of this system (Figure 6.2) has 30 buses (nodes) and 41 transmission lines (links), i.e. number of components $N = 71$. These 30 buses that are represented as nodes can be either generator nodes, transmission nodes or demand nodes. For demonstration purposes, the generation capacity of all generator nodes is set to 60 MW, each demand node requests 20 MW, and transmission lines capacities are 50MW, which will be represented as link capacities.

For a given earthquake hazard, the survival probabilities of the components

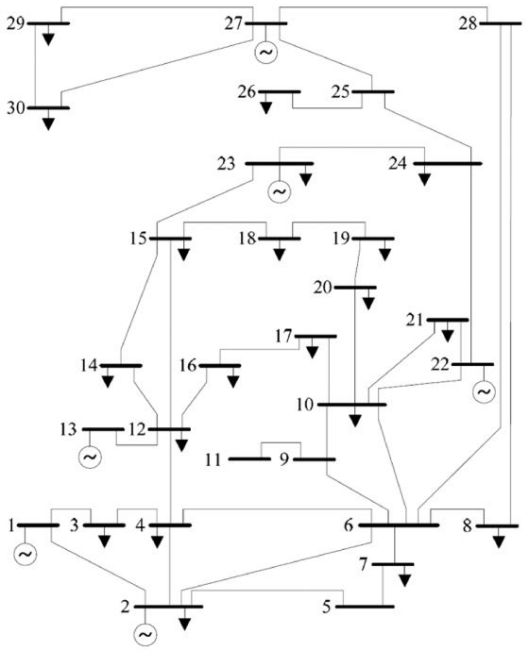

Figure 6.1: Single-line diagram of the IEEE 30-bus test system [2].

are known, which will be assumed as 0.8 for generator nodes, 0.85 for demand nodes, 0.85 for transmission nodes, and 0.8 for transmission links. The levels of improvement will be also assumed to be different for each type of component: generator nodes can only be improved to one level of survival probability (0.87) at the cost of $350,000; demand nodes can be improved to two levels of survival probability (0.9, 0.95) at the cost of $50,000 and $70,000, respectively; transmission nodes can be improved to three levels of survival probability (0.9, 0.95, 0.97) at the cost of $15,000, $30,000 and $50,000, respectively; finally, transmission lines can be improved to two levels of survival probability (0.85, 0.93) at the cost of $35,000 and $50,000. This information is summarized in Figure 6.3.

The objective is to maximize the expected post-disaster electric demand met, which in the simplified graph from Figure 6.2 can be calculated by solving

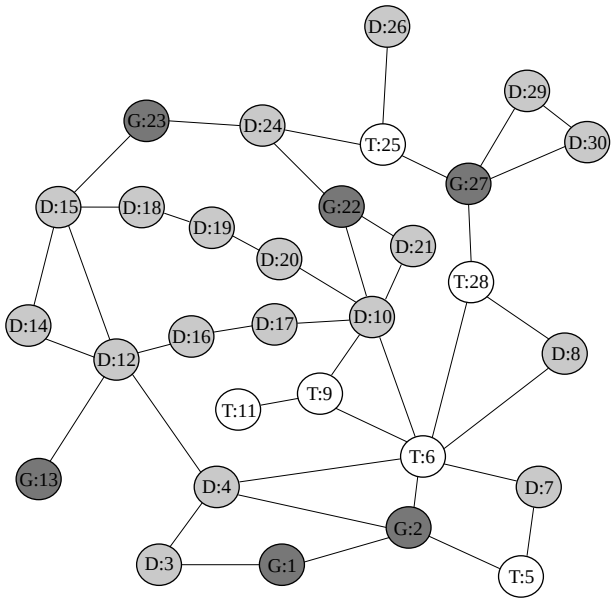

Figure 6.2: Graph representation of the IEEE 30-bus test system [2]. The dark grey nodes labeled with G represent the generator nodes, the white nodes labeled with T represent transmission nodes, and the light grey nodes labeled with D represent the demand nodes.

a max flow problem, which needs to connect all generator nodes to a source node, and all demand nodes to a sink node. This performance metric will be depicted as F and its value when the network is healthy is 350 MW.

Four constraint cases for long-term mitigation are studied separately. They are motivated by real-world limitations and selected to use the mathematical constraints described in 4.2.4. Case 3 and Case 4 are complicated decision making scenarios that the proposed approach can handle.

Case 1 Budget of $300,000.

Case 2 Budget of $700,000.

Case 3 Budget of $700,000. No demand nodes can be improved.

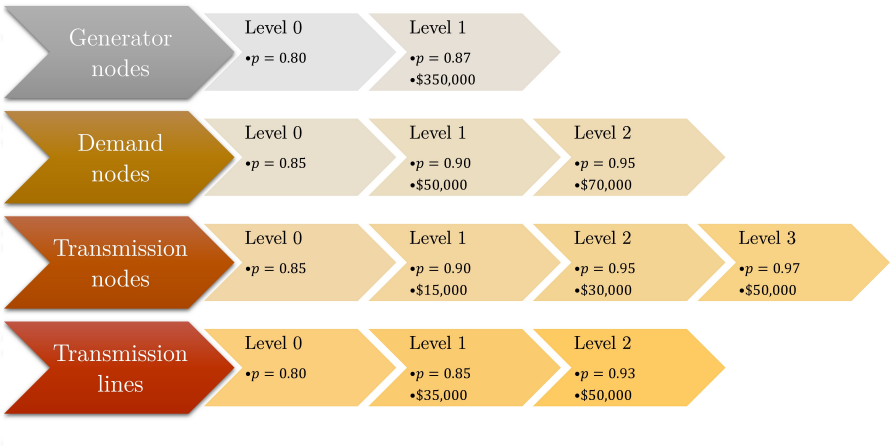

Figure 6.3: Levels of improvement with associated survival probabilities and costs for each type of component.

Case 4 Budget of $700,000. The political decision of improving nodes G:22 and G:23 has been irreversible made without technical consultation.

A CIM ranking based on impact is presented to provide a better understanding of the individual effects of isolated failures in the network. The delta centrality that is derived from using the demand met as performance metric is denoted as $C_i^{\Delta F} = (\Delta F)_i/F$. Table 6.1 presents a summary of this delta centrality results for the IEEE 30-bus test system. Note that the most impactful elements are the generators, subsequently, generator 13 and its adjacent link and demand node have the same centrality value of 0.1429. The rest of the nodes and links have little to none impact when failing in isolation. However, this should not be interpreted as they are not important because there may be simultaneous component failures that are both probable and impactful, as discussed in Chapter 3.

Table 6.1: Component ID sorted by $C_i^{\Delta F}$.

Components	$C_i^{\Delta F}$
G:2	0.2000
G:1, G:22, G:23, G:27	0.1714
D:12, G:13, (D:12, G:13)	0.1429
D:10, D:15	0.0571
D:3, D:4, T:6, D:19, D:24, T:25, (G:1, D:3), (D:15, G:23)	0.0286
Rest (53 components)	0.0000

6.2. Application of Methodology

6.2.1 Data Generation and Transformation

Probable failures patterns are constructed using Monte Carlo Simulation based on the baseline component survival probabilities. The computation of the selected performance metric (demand met via solving the max flow problem) is calculated in polynomial time, therefore, there is no constraint to work with as many failure patterns as desired.

For this example, the prediction boundaries for each type of component are different. The analysis to select η should be done using Equation (4.1) for components that have the same lower predict bound because they share the same mean for their Gaussian curve. Note that generator nodes and transmission lines share the baseline probability of 0.8, which means that the range of prediction for both will start at 0.8. On the other hand, transmission lines can be improved to a higher probability than the generators. Thus, the upper boundary for transmission lines will have fewer data points than the upper boundary for generator nodes. Therefore, it is enough to analyze the type of

component with the higher range of prediction, which are the transmission lines.

$$0.93 - 0.80 \leq 2 \cdot \sqrt{0.80 \cdot 0.20/\eta}$$

$$\eta \leq 37.87$$

Similarly, demand nodes and transmission nodes share the same baseline probability: 0.85. The highest upper prediction boundary is for transmission nodes, so we apply Equation (4.1) on those components.

$$0.97 - 0.85 \leq 2 \cdot \sqrt{0.85 \cdot 0.15/\eta}$$

$$\eta \leq 35.41$$

Considering these two upper bounds for η, we select $\eta = 35$. This is the size of the sample to take from the realization dataset to generate the probabilistic dataset. An example of the histogram for each type of component is represented in Figure 6.4.

6.2.2 Statistical Modeling

A random forest is used as the statistical learning model to learn the complex relationships embedded in the probabilistic dataset. First, this probabilistic dataset (20,000 observations) is divided in two: train set (80%) and test set (20%). To select appropriate parameters for this random forest model, a cross-validation with $k = 5$ is performed within the train set with the hyperparameter grid described in Table 6.2.

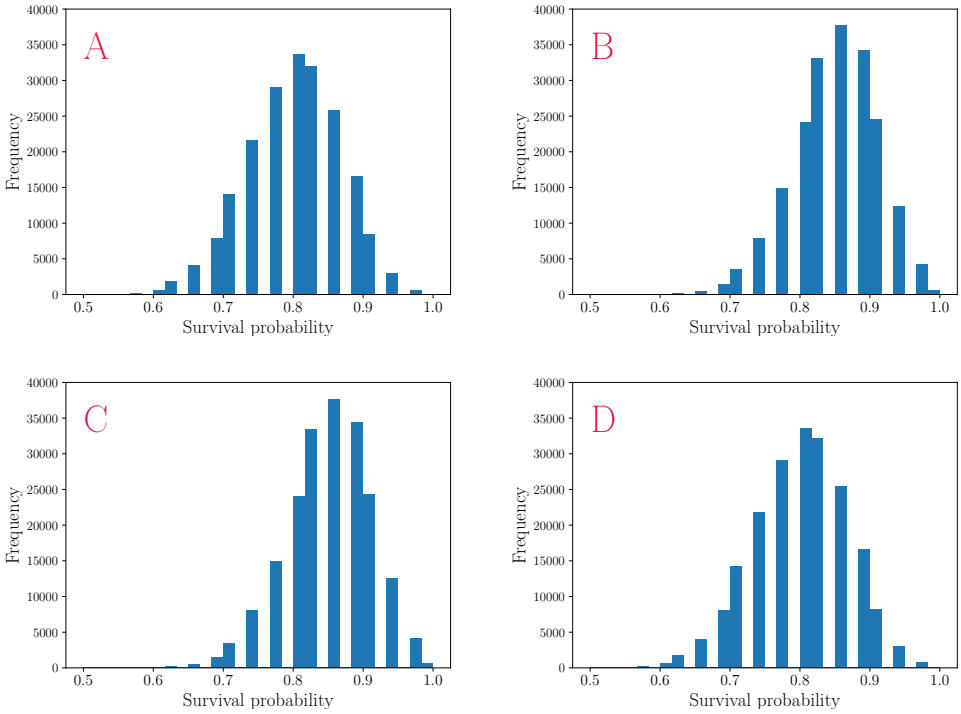

Figure 6.4: Histograms of component survival probabilities generated with $\eta = 35$ for each type of component. A: generator nodes; B: demand nodes; C: transmission node; D: transmission link.

In Table 6.2, the number of estimators is the number of trees that are going to be part of the ensemble. The maximum depth controls the depth of each tree in the ensemble. The maximum number of features on split is the number of features that will be considered in each split. In the case of the N option, it considers all the features for split. In the case of the $\sqrt{N}$ option, it considers a number of features equal to the square root of the total number of features. The metric used to tune these hyper-parameters is the mean squared error (MSE).

With the tuned hyper-parameters (shown in bold in Table 5.1), a learning curve (Figure 6.5) is built running 5-fold cross-validation repeatedly for several training set sizes. It can be noted in Figure 6.5 that the current random forest

Table 6.2: Hyper-parameter values considered in tunning the random forest. Selected in bold.

Hyper-parameter	Values
No. of estimators	200, 400, 600, 800, 1000, 1200, 1400, 1600, **1800**, 2000
Maximum depth	10, 20, 30, 40, 50, 60, 70, 80, 90, **100**, None
Max. features on split	$\mathbf{N}, \sqrt{N}$

model has a low training error compared with the validation error, which is a sign of overfitting. In this cases, it is recommended to reduce the complexity of the model using regularization. For this specific random forest, the parameter maximum observation per leaf node is selected as a regularization parameter. After experimenting with several values for this parameter, we select to set it to be 500 (based on its validation error). The learning curves after with this regularization are now closer, which suggests that the new model is less biased and apt for better generalization.

In addition, from this learning curve, it can be noted that a size of 5,000 is necessary to avoid overestimation of the validation error. This result tell us two things: (1) using 5,000 samples for training in cross-validation should be ensured to get a proper error estimation for tuning; (2) to meet the requirement in (1) with 5-fold cross validation, it is needed to have at least $5,000 \times 5/4 = 6250$ samples for training. Therefore, we do not need to use the 16,000 samples that were initially generated by the probabilistic transformation.

The final model is build with the parameters from the cross-validation and regularization. Its performance metrics mean squared error (MSE) and mean absolute error (MAE) were 51.8783 and 5.7398 respectively. To have other assessment of the quality of the model, we made a reliability curve for the

test set shown in Figure 5.5, where the closest the red line is to the gray dashed, the lower the bias error. This curve answers the question: "Given a predicted average $\bar{\varphi}_p$, what is the most likely observation of the actual $\bar{\varphi}$?" It can be noted that the extremes have high bias error, therefore, it should be expected that those those values the prediction is more likely to be off by either overestimating (lower extreme) or underestimating (upper extreme) the actual average performance metric.

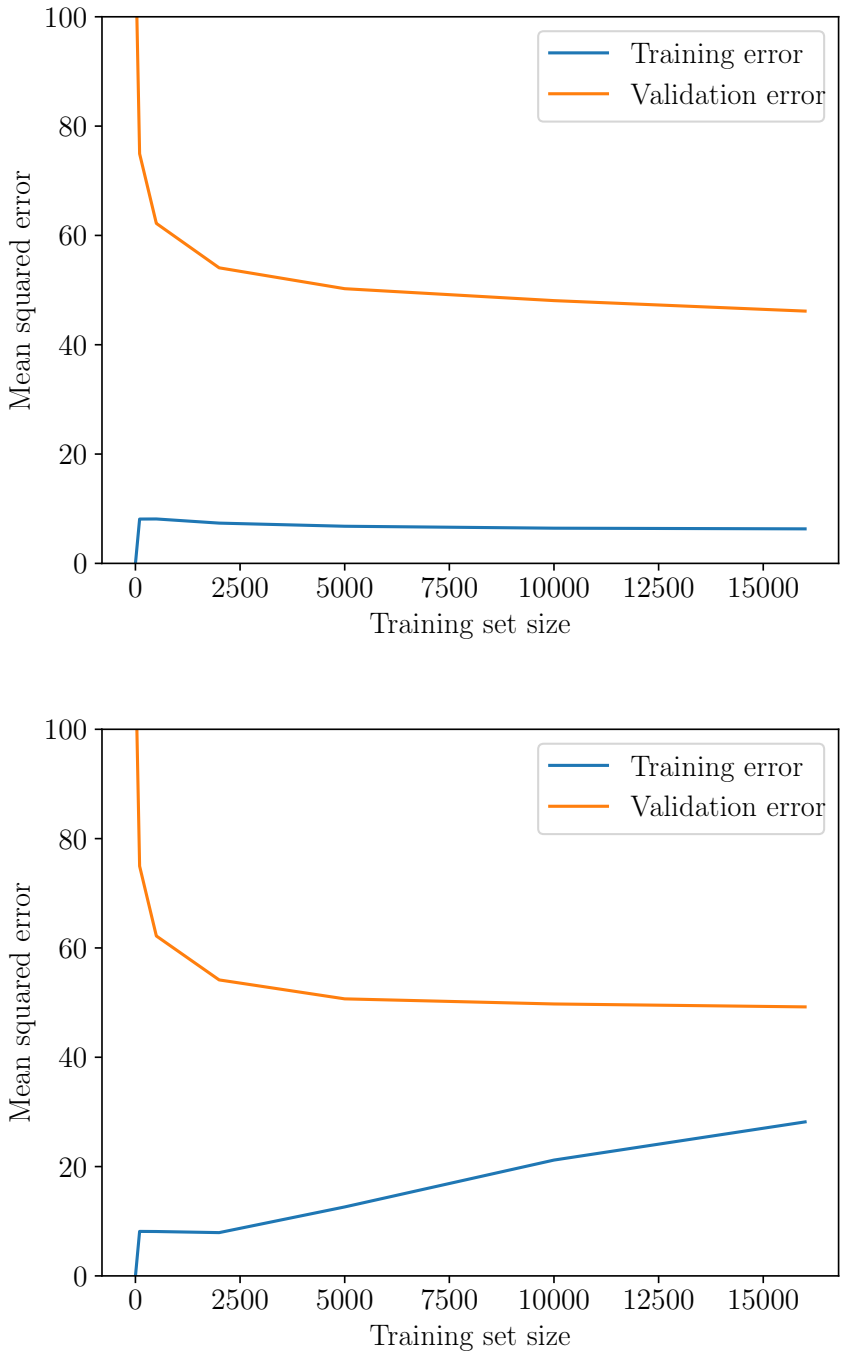

Figure 6.5: Learning curve for random forest model before (above) and after (below) regularization.

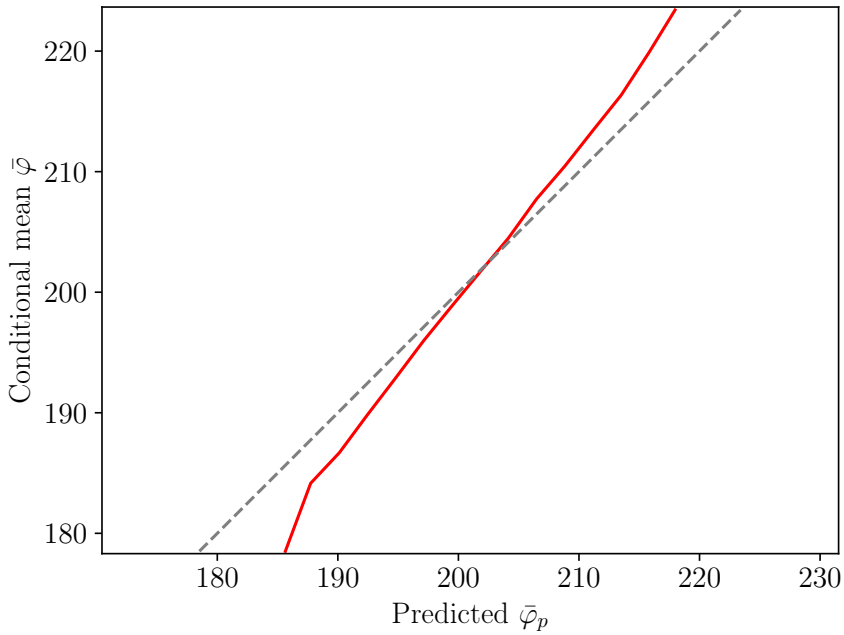

Figure 6.6: Reliability curve for final random forest model. Gray dashed line is a perfect reliability curve. Red is actual.

6.2.3 Optimization

A genetic algorithm is used to find near optimal solutions in the probabilistic space using the previous machine learning model to estimate the expected value of the performance metric for each improvement strategy. The selected parameters are presented in Table 6.3.

Table 6.3: Genetic algorithm parameters.

Parameter	Value
Cross-over probability	0.5
Mutation probability	0.2
No. of Generations	500
Population Size	800

In Table 6.3, the cross-over probability is the likelihood of two parent solutions to be combined to get new children solutions; otherwise, they will not change. This probability is suggested to be set to 0.5 [45]. The mutation probability is associated to changing one of the chromosomes of children solutions. The number of generations sets how many times old population are going to perish to give birth to new ones. Finally, the population size is the number of individuals (solutions) in each generation. The last three parameters are set via empirical analysis.

In order to run the genetic algorithm with the selected parameters, the constraints must be defined. Each constrain case is related to a mathematical constraint introduced in Section 4.2.4 in the following manner.

Case 1 Set Budget = $\$300,000$ in Constraint (4.3)

Case 2 Set Budget = $\$700,000$ in Constraint (4.3)

Case 3 Set Budget = $\$700,000$ in Constraint (4.3) and set $l_i = 0$ for all demand nodes in Constraint (4.4)

Case 4 Set Budget = $\$700,000$ in Constraint (4.3) and set $x_i = 1$ for generator nodes G:22 and G:23 (level 1 is the maximum improvement for generator nodes), i.e. all solutions to be explored will be generated setting $x_i = 1$ for those generator nodes

Constraint case 4 cannot be handled with any of the constraints presented in Section 4.2.4. It requires to code the restriction directly to the genetic algorithm. Finally, the function $cost(\mathbf{x})$ from Constraint (4.3) is non-linear for this problem, thus, it can be coded as a look-up table.

6.2.4 Correction of Predicted Performance Metric $\hat{\varphi}_p$

In Equation (4.9), $Z_{1-(\alpha/2)}$ for level of significance $\alpha = 0.05$ will take $Z_{0.975} = 1.96$. Then, we decide to have a level of error of $\epsilon = 1\%$. Taking $m = 1000$, we can calculate the average performance metric $\bar{\varphi}_m$ and the standard deviation for the performance metric s_m for each of the solutions. The following is an extract of the best solutions for each constraint case. Remind that for each constraint case there were several runs of the genetic algorithm to ensure get several local optima. Each of these local optima has to be corrected.

Case 1 $\bar{\varphi}_m = 219.48$ and $s_m = 53.85$ result in $n' \geq 2,312.96$

Case 2 $\bar{\varphi}_m = 230.58$ and $s_m = 53.69$ result in $n' \geq 2,082.83$

Case 3 $\bar{\varphi}_m = 221.17$ and $s_m = 54.47$ result in $n' \geq 2,330.10$

Case 4 $\bar{\varphi}_m = 234.66$ and $s_m = 53.22$ result in $n' \geq 1,975.99$

Looking at the lower bounds for n' for each constraint case, the final value selected for n' is **2,500** for all of the corrections. The corrected values using this n' are presented in Table 6.4.

6.3. Results and Discussion

In Case 1, because of the restrictive budget, improving a generator node is not possible, thus, the solution must be a combination of other types of components. The solution $\mathbf{x}^{*(1)}$ suggests to prioritize some components that are close to generators, while other components were selected due to their strategic position to reach other demand nodes (e.g. T:6). This selection is intuitive because they are components needed to distribute electricity to other demand nodes. In Case 2, when budget increases to $700,000, there are enough resources to enhance a generator, but other components are prioritized because their combination is found to be more effective to minimize impact (i.e. even with a high individual impact, generator nodes are not the first option for improvement). The solution suggested includes all improvements from Case 1 along with others that share the proximity to generator nodes and a $C^{\Delta F}$ value higher than 0 (e.g. D:24). Nevertheless, others are less intuitive when looking at its position and $C^{\Delta F}$ value (e.g. link T:9).

In Case 3, the budget level is maintained but no demand nodes can be improved due to an external reason. Say, for example, that the delivering time for devices needed to enhance demand nodes is too long for the desired planning schedule. This constraint mandates that the resources previously invested in demand

Table 6.4: Solutions for constrained cases with component ID sorted by component type and index number. Each solution column contains the level of improvement suggested for each component. At the bottom, predicted average performance metric $\bar{\varphi}_p$ (objective) and corrected expected performance metric $\bar{\varphi}_c$ for each solution. Note that from the 71 components, only the ones that have improvements are presented.

Component	Solution $\mathbf{x}^{*(j)}$ to constraint case j			
i	$x_i^{*(1)}$	$x_i^{*(2)}$	$x_i^{*(3)}$	$x_i^{*(4)}$
G:27	0	0	**1**	0
D:4	**2**	**2**	0	**2**
D:10	**2**	**2**	0	**2**
D:12	**2**	**2**	0	**2**
D:15	**2**	**2**	0	0
D:19	0	**1**	0	0
D:24	0	**2**	0	0
T:6	**2**	**2**	**2**	0
T:9	0	**2**	0	0
T:25	0	**2**	**2**	**2**
T:28	0	0	**2**	0
(G:1, D:3)	0	**2**	**2**	**2**
(G:2, T:6)	0	0	**2**	0
(D:4, D:12)	0	0	0	**2**
(D:10, D:20)	0	**2**	0	0
(D:10, G:22)	0	0	**2**	0
(D:12, G:13)	**2**	**2**	**2**	**2**
(D:15, G:23)	0	**2**	**2**	**2**
(G:27, D:29)	0	0	0	**2**
$\bar{\varphi}_p$ (predicted)	208.73	209.41	208.99	213.11
$\bar{\varphi}_c$ (corrected)	218.57	230.71	221.14	234.38
Thous. of USD spent	290	690	690	690

nodes have to go to other type of components. Our method is straightforward in handling this constraint: the only modification is to set to zero l_i for all demand nodes. Only after this restriction, the method finds suitable to invest in improving an expensive generator node.

In the final case in which nodes G:22 and G:23 have been decided to be invested, and the budget remains \$700,000 (as Case 2), the solution suggest to remove the investment on some components close to G:22 and G:23 (e.g. D:15, D:19, D:24), and allocate the resources in farther areas (e.g. links (D:4, D:12), (G:27, D:29)) that are more vulnerable. In other words, the method finds out that after these two close generators were enhanced, the area where they are located is now less vulnerable than other areas in the network. Therefore, the reward is higher when allocating the money in components that were not considered in the solution of Case 2.

For all of the cases presented, the absolute difference between $\bar{\varphi}_p$ and the $\bar{\varphi}_c$ is higher than the expected MAE (5.7398). The reason for this is the following. The MAE is calculated only for the regression model, and the error in $\bar{\varphi}_p$ comes from two sources: sampling error (9.0993 calculated using Equation (4.8)) and the statistical model error (7.2026). Hence, it should not be a surprise to have this difference out of the MAE range. It is worth reporting that from our experiments with different seeds for the genetic algorithm and correcting several different solutions for each case, it is noticed that the estimates of $\bar{\varphi}_p$ for this problem presented a strong correlation with $\bar{\varphi}_c$, which provides support to say that the statistical model is useful for exploring the solution space.

Chapter 7

Conclusions

This work discussed and expanded two methods for mitigation decision making in physical networks with an emphasis in including both uncertainty and complexity of network failure. The probabilistic delta centrality, a novel centrality measure that accounts for failure probabilities, shows how the expected impact of components failures—that changes with their probability of failure—does not correspond with individual and synergistic delta centralities. Therefore, using these component importance measures would provide sub-optimal improvement strategies. Consequently, when there is stochastic information available, our data-based methodology is a better option. Our data-based methodology leverages the realistic failure pattern data and converts this to a probabilistic real-valued space through sampling to then employ in a novel manner statistical learning models to estimate the function f, which captures both uncertainty and complexity embedded in the network failure phenomena like hazard intensities, hazard characteristics, failure correlations, and dependencies among components. This function then becomes the objective

in a problem suitable for constrained decision-making using mathematical optimization or metaheuristic search techniques. The two examples presented showed its flexibility in incorporating complexity, and in handling intricate constraints.

Chapter 8

Future work

We envision that our data-based approach can be extended to solve other type of stochastic network mitigation problems. For example, influence maximization in social networks could be assisted with our approach either using simulated data obtained from contagion models. To implement this, a type of event should be identified and simulated so that the state of the network after the event can be expressed as a binary vector. Then, using the procedure presented in this thesis, it can assist decisions regarding increasing the probabilities of a node to be influenced.

In addition, we consider to be a useful extension to convert failure states from a binary representation to a either discrete or continuous. From our experience working with civil engineers, current Monte Carlo simulations are able to provide discrete damage states. An example of using this information to calculate the performance metric is when we have a network of bridges. For instance, their capacity could decrease to 90% of their max capacity when damage is slight, or to 0% when damage is extensive.

References

[1] D. Brockmann, D. Helbing, The Hidden Geometry of Complex, Network-Driven Contagion Phenomena, Science 342 (6164) (2013) 1337 LP – 1342.

[2] Y.-P. Fang, N. Pedroni, E. Zio, Resilience-Based Component Importance Measures for Critical Infrastructure Network Systems, IEEE Transactions on Reliability 65 (2) (2016) 502–512. doi:10.1109/TR.2016.2521761.

[3] ASCE, 2017 infrastructure report card: A comprehensive assessment of America's infrastructure (2017).

[4] Mitigation of malicious attacks on networks., Proceedings of the National Academy of Sciences of the United States of America 108 (10) (2011) 3838–41. doi:10.1073/pnas.1009440108.

[5] X. Wu, D. Sheldon, S. Zilberstein, Optimizing Resilience in Large Scale Networks, Proceedings of the Thirtieth AAAI Conference on Artificial Intelligence (AAAI-16) (2016) 3922–3928.

[6] S. I. Lim, S. J. Lee, M. S. Choi, D. J. Lim, B. N. Ha, Service restoration methodology for multiple fault case in distribution systems, IEEE Transactions on Power Systems 21 (4) (2006) 1638–1644. doi:10.1109/TPWRS.2006.879275.

[7] Y. Wang, C. Chen, J. Wang, R. Baldick, Research on Resilience of Power Systems Under Natural Disasters - A Review, IEEE Transactions on Power Systems 31 (2) (2015) 1–10. doi:10.1109/TPWRS.2015.2429656.

[8] P. Suarez, W. Anderson, V. Mahal, T. R. Lakshmanan, Impacts of flooding and climate change on urban transportation: A systemwide performance assessment of the Boston Metro Area, Transportation Research Part D: Transport and Environment 10 (3) (2005) 231–244. doi:10.1016/j.trd.2005.04.007.

[9] P. M. Murray-Tuite, X. Fei, A Methodology for assessing transportation network terrorism risk with attacker and defender interactions, Computer-Aided Civil and Infrastructure Engineering 25 (6) (2010) 396–410. doi:10.1111/j.1467-8667.2010.00655.x.

[10] D. E. Alexander, Principles of emergency planning and management, Oxford University Press on Demand, 2002. doi:10.1136/hrt.2004.040329.

[11] M. G. Whitman, K. Barker, J. Johansson, M. Darayi, Component importance for multi-commodity networks: Application in the Swedish railway, Computers and Industrial Engineering 112 (2017) 274–288. doi:10.1016/j.cie.2017.08.004.

[12] W. Zhang, N. Wang, Resilience-based risk mitigation for road networks, Structural Safety 62 (2016) 57–65. doi:10.1016/j.strusafe.2016.06.003.

[13] M. Sánchez-Silva, M. Daniels, G. Lleras, D. Patino, A transport network reliability model for the efficient assignment of resources, Transportation

Research Part B: Methodological 39 (1) (2005) 47–63. doi:10.1016/j.trb.2004.03.002.

[14] C. D. Nicholson, K. Barker, J. E. Ramirez-Marquez, Flow-based vulnerability measures for network component importance: Experimentation with preparedness planning, Reliability Engineering and System Safety 145 (2016) 62–73. doi:10.1016/j.ress.2015.08.014.

[15] E. Hernández-Perdomo, C. M. Rocco, J. E. Ramirez-Marquez, Node ranking for network topology-based cascade models - An Ordered Weighted Averaging operators' approach, Reliability Engineering and System Safety 155 (2016) 115–123. doi:10.1016/j.ress.2016.06.014.

[16] H. Y. Yin, L. Q. Xu, Measuring the structural vulnerability of road network: A network efficiency perspective, Journal of Shanghai Jiaotong University (Science) 15 (6) (2010) 736–742. doi:10.1007/s12204-010-1078-z.

[17] H. Cai, J. Zhu, C. Yang, W. Fan, T. Xu, Vulnerability Analysis of Metro Network Incorporating Flow Impact and Capacity Constraint after a Disaster, Journal of Urban Planning and Development 143 (2) (2017) 1–10. doi:10.1061/(ASCE)UP.1943-5444.0000368.

[18] E. Jenelius, L. G. Mattsson, Road network vulnerability analysis: Conceptualization, implementation and application, Computers, Environment and Urban Systems 49 (2015) 136–147. doi:10.1016/j.compenvurbsys.2014.02.003.

[19] X. Wu, Stochastic Network Design: Models and Scalable Algorithms, Ph.D. thesis (jan 2016). doi:816.

[20] A. J. Kleywegt, A. Shapiro, T. Homem-de Mello, The Sample Average Approximation Method for Stochastic Discrete Optimization, SIAM Journal on Optimization 12 (2) (2002) 479–502. doi:10.1137/S1052623499363220.

[21] S. Peeta, F. Sibel Salman, D. Gunnec, K. Viswanath, Pre-disaster investment decisions for strengthening a highway network, Computers and Operations Research 37 (10) (2010) 1708–1719. doi:10.1016/j.cor.2009.12.006.

[22] A. Shapiro, Monte Carlo Sampling Methods, Handbooks in Operations Research and Management Science 10 (2003) 353–425. doi:10.1016/S0927-0507(03)10006-0.

[23] P. Lin, N. Wang, Stochastic post-disaster functionality recovery of community building portfolios I: Modeling, Structural Safetydoi:10.1016/j.strusafe.2017.05.002.

[24] S. Rinaldi, J. Peerenboom, T. Kelly, Identifying, understanding, and analyzing critical infrastructure interdependencies, IEEE Control Systems Magazine 21 (6) (2001) 11–25. doi:10.1109/37.969131.

[25] R. Lee, A. S. Kiremidjian, Uncertainty and correlation for loss assessment of spatially distributed systems, Earthquake Spectra 23 (4) (2007) 753–770. doi:10.1193/1.2791001.

[26] M. Ouyang, Z. Pan, L. Hong, L. Zhao, Correlation analysis of different vulnerability metrics on power grids, Physica A: Statistical Mechanics and its Applications 396 (2014) 204–211. doi:10.1016/j.physa.2013.10.041.

[27] F. Rupi, S. Angelini, S. Bernardi, A. Danesi, G. Rossi, Ranking links in a road transport network: A practical method for the calculation of link importance, Transportation Research Procedia 5 (2015) 221–232. doi:10.1016/j.trpro.2015.01.003.

[28] V. Latora, M. Marchiori, Vulnerability and protection of infrastructure networks, Physical Review E - Statistical, Nonlinear, and Soft Matter Physics 71 (1) (2005) 1–4. doi:10.1103/PhysRevE.71.015103.

[29] E. L. d. Oliveira, L. d. S. Portugal, W. P. Junior, Determining Critical Links in a Road Network: Vulnerability and Congestion Indicators, Procedia - Social and Behavioral Sciences 162 (Panam) (2014) 158–167. doi:10.1016/j.sbspro.2014.12.196.

[30] C. Balijepalli, O. Oppong, Measuring vulnerability of road network considering the extent of serviceability of critical road links in urban areas, Journal of Transport Geography 39 (2014) 145–155. doi:10.1016/j.jtrangeo.2014.06.025.

[31] W. H. Ip, D. Wang, Resilience and friability of transportation networks: Evaluation, analysis and optimization, IEEE Systems Journal 5 (2) (2011) 189–198. doi:10.1109/JSYST.2010.2096670.

[32] Q. Qiang, A. Nagurney, A unified network performance measure with importance identification and the ranking of network components, Optimization Letters 2 (1) (2008) 127–142. doi:10.1007/s11590-007-0049-2.

[33] H. Jönsson, J. Johansson, H. Johansson, Identifying critical components in technical infrastructure networks, Proceedings of the Institution of Me-

chanical Engineers, Part O: Journal of Risk and Reliability 222 (2) (2008) 235–243. doi:10.1243/1748006XJRR138.

[34] A. T. Murray, T. C. Matisziw, T. H. Grubesic, A Methodological Overview of Network Vulnerability Analysis, Growth and Change 39 (4) (2008) 573–592.

[35] X. Wu, Y. Xue, B. Selman, C. P. Gomes, XOR-Sampling for Network Design with Correlated Stochastic Events (3). arXiv:1705.08218.

[36] M. Wang, T. Takada, Macrospatial Correlation Model of Seismic Ground Motions, Earthquake Spectra 21 (4) (2005) 1137–1156. doi:10.1193/1.2083887.

[37] V. Latora, M. Marchiori, Efficient Behavior of Small-World Networks, Physical review letters 87 (19) (2001) 198701. doi:10.1103/PhysRevLett.87.198701.

[38] V. Latora, M. Marchiori, A measure of centrality based on network efficiency, New Journal of Physics 9. doi:10.1088/1367-2630/9/6/188.

[39] K. Atkins, J. Chen, V. S. A. Kumar, A. Marathe, The structure of electrical networks: a graph theory based analysis, International Journal of Critical Infrastructures 5 (3) (2009) 265–284. doi:10.1504/IJCIS.2009.024874.

[40] Z. Wang, A. Scaglione, R. J. Thomas, Generating Statistically Correct Random Topologies for Testing Smart Grid Communication and Control Networks, IEEE Transactions on Smart Grid 1 (1) (2010) 28–39. doi:10.1109/TSG.2010.2044814.

[41] J. E. Padgett, R. DesRoches, Methodology for the development of analytical fragility curves for retrofitted bridges, Earthquake Engineering & Structural Dynamics 37 (8) (2008) 1157–1174. doi:10.1002/eqe.801.

[42] R. Faturechi, E. Miller-Hooks, Travel time resilience of roadway networks under disaster, Transportation Research Part B: Methodological 70 (2014) 47–64.

[43] W. Zhang, C. Nicholson, A multi-objective optimization model for retrofit strategies to mitigate direct economic loss and population dislocation, Sustainable and Resilient Infrastructure 1 (3-4) (2016) 123–136. doi:10.1080/23789689.2016.1254995.

[44] A. Chen, H. Yang, H. K. Lo, W. H. Tang, Capacity reliability of a road network: an assessment methodology and numerical results, Transportation Research Part B: Methodological 36 (3) (2002) 225–252. doi:10.1016/S0191-2615(00)00048-5.

[45] K. Deb, Multi-objective optimization using evolutionary algorithms, John Wiley & Sons, 2001.

[46] Power Systems Test Case Archive - UWEE.
URL https://www2.ee.washington.edu/research/pstca/